

Optical variability properties of high luminosity AGN classes

C. S. Stalin^{1,2}, Gopal-Krishna², Ram Sagar¹ and Paul J. Wiita³

¹ State Observatory, Manora Peak Nainital-263 129

² National Centre for Radio Astrophysics, TIFR, Pune University Campus, Pune-411 007

³ Department of Physics & Astronomy, MSC 8R0314, Georgia State University, Atlanta, Georgia 30303-3088, USA

Address for correspondence:

Prof. Ram Sagar
State Observatory
Manora Peak
Nainital - 263 129
Phone : (05942) 235136, 235583
Fax : (05942) 235136
Email : sagar@upso.ernet.in
: ram_sagar0@yahoo.co.in

Abstract

We present the results of a comparative study of the intra-night optical variability (INOV) characteristics of radio-loud and radio-quiet quasars, which involves a systematic intra-night optical monitoring of seven sets of high luminosity AGNs covering the redshift range $z \simeq 0.2$ to $z \simeq 2.2$. The sample, matched in the optical luminosity – redshift ($M_B - z$) plane, consists of seven radio-quiet quasars (RQQs), eight radio lobe-dominated quasars (LDQs), six radio core-dominated quasars (CDQs) and five BL Lac objects (BLs). Systematic CCD observations, aided by a careful data analysis procedure, have allowed us to detect INOV with amplitudes as low as 1%. Present observations cover a total of 113 nights (720 hours) with only a single quasar monitored as continuously as possible on a night. Considering cases of only unambiguous detections of INOV we have estimated duty cycles (DCs) of 17%, 12%, 20% and 72% respectively for RQQs, LDQs, CDQs, and BLs. The low amplitude and low DC of INOV shown by RQQs compared to BLs can be understood in terms of their having optical synchrotron jets which are modestly misdirected from us. From our fairly extensive dataset, no unambiguous general trend of a correlation between the INOV amplitude and the apparent optical brightness of the quasar is noticed. This suggests that the physical mechanisms of INOV and long term optical variability (LTOV) do not have a one-to-one relationship and different factors are involved. Also, the absence of a clear negative correlation between the INOV and LTOV characteristics of blazars of our sample points towards an inconspicuous contribution of accretion disk fluctuations to the observed INOV. The INOV duty cycle of the AGNs observed in this program suggests that INOV is associated predominantly with highly polarised optical components. We also report new VLA imaging of two RQQs (1029+329 & 1252+020) in our sample which has yielded a 5 GHz detection of one of them (1252+020; $S = 1$ mJy).

keywords: galaxies: active — galaxies: jets — galaxies: photometry — quasars:general.

1 Introduction

The question of why only a small fraction of quasars are radio-loud has been debated for almost forty years. Various arguments have been put forward to explain this apparent radio-loud/radio-quiet dichotomy. Although the reality of the dichotomy has even been questioned (e.g., Goldschmidt et al. 1999; White et al. 2000), the most careful analysis of the tricky selection effects indicates that it is real (Ivezic et al. 2002). It has been argued recently that the radio emission correlates with the mass of the nuclear black hole (e.g., Dunlop et al. 2003 and references therein); however, this assertion has been questioned (Ho 2002; Woo & Urry 2002). McLure & Dunlop (2001) stress the importance of accretion rate and possible changes in accretion mode to this dichotomy.

On the theoretical side, two main approaches have been put forward to explain this dichotomy. In one scenario, the jets in RQQs are absent or inherently weak. Some possible mechanisms identify this differentiating factor with the spin of the black hole (Wilson & Colbert 1995, Blandford 2000), or magnetic configurations (Meier 2002). At the other extreme lies the hypothesis that the relativistic jets in RQQs are largely snuffed out before escaping the nuclear region itself due to heavy Inverse Compton losses (Kundt 2002). As a consequence, jets on radio emitting physical scales are quenched, even though they might emit substantial amounts of non-thermal optical synchrotron emission on micro-arc second scales. Unfortunately, such micro-arcsec scales are beyond the reach of any existing imaging telescopes and the only way to probe the conditions at such small scales is through flux variability observations.

Though intra-night optical variability (INOV) was convincingly established for blazars over a decade ago (Miller, Carini & Goodrich 1989), the question of whether RQQs too show INOV has remained controversial (Gopal-Krishna et al. 1995, 2000; Jang & Miller 1995, 1997; Rabbette et al. 1998, de Diego et al. 1998; Romero et al. 1999). The cause of INOV is still a much debated issue. However, for blazars (CDQs and BL Lacs) which are believed to be dominated by non-thermal Doppler boosted emission from jets (e.g., Blandford & Rees 1978), the occurrence of rapid intensity variations in both the radio and optical are believed to be due to shocks propagating down their relativistic jets (e.g., Marscher & Gear 1985). Intra-night variability in blazars may well arise from instabilities or fluctuations in the flow of such jets (e.g., Hughes, Aller & Aller 1992; Marscher, Gear & Travis 1992). Still, alternate models, which invokes accretion disk instabilities or perturbations (e.g., Mangalam & Wiita 1993; for a review see Wiita 1996) may also explain INOV, particularly in RQQs where any contribution from the jets, if they are at all present, is weak.

While conclusive evidence for the presence of jets in RQQs is far from clear, deep VLA observations hint at the presence of weak jets even in RQQs (Kellermann et al. 1989; Miller, Rawlings & Saunders 1993; Kellermann et al. 1994; Papadopoulos et al. 1995; Kukula et al. 1998; Blundell & Beasley 1998; Blundell & Rawlings 2001). The existence of insipient nuclear jets in RQQs have also been inferred from radio spectral index measurements of optically selected quasar samples (Falcke, Patnaik & Sherwood 1996). If indeed optical synchrotron jets exists even in RQQs, then a fairly robust signature of such un-imageable (micro-arc scale) jets can come from

detection of INOV at the level exhibited by their radio loud counterparts, namely the LDQs. In the light of the above discussions, a project to search for INOV in the four major classes of powerful AGNs was initiated in 1998 as a collaborative effort between the State Observatory, Nainital and the National Centre for Radio Astrophysics (NCRA), Pune. The present paper presents many of the detailed results of this project. Some of these results from this large project are published elsewhere (Gopal-Krishna et al. 2003, hereafter GSSW03; Stalin et al. 2003, SGSW03; Sagar et al. 2003, SSGW03).

2 Selection of the sample

AGNs in general have very different observational characteristics including a huge range in luminosity, redshift and powers across the electromagnetic spectrum. Also, the co-moving number density of quasars detected at a given absolute magnitude is found to undergo a rapid evolution with redshift (Schmidt & Green 1983; Boyle et al. 2000; Wisotzki 2000). Therefore, sample selection is crucial for studying INOV of quasars. To avoid selection biases introduced by differences in luminosity and redshift, the objects were selected such that all objects in a given set have similar optical magnitudes, in addition to having very similar redshifts and they are thus well matched in the optical luminosity–redshift plane. Our sample, selected from the catalog of Véron-Cetty & Véron (1998), consists of seven sets of AGNs covering a total redshift range from $z = 0.17$ to $z = 2.2$. Each set consists of a radio-quiet quasar (RQQ), a radio lobe-dominated quasar (LDQ), a radio core-dominated quasar (CDQ)/or a BL Lac object (BL). These seven sets cover seven narrow redshift intervals centered at $z = 0.21, 0.26, 0.35, 0.43, 0.51, 0.95$ and 1.92 .

Our sample of luminous, *bonafide* quasars ($-30.0 < M_B < -24.3$ mag), thus overcome the selection biases such as K-correction, evolutionary effects and any other differences introduced due to luminosity and redshift. Further, so as to have only *bona fide* RQQs in the sample, only those objects having a radio flux ≤ 1 mJy at 5 GHz were selected.

Our entire sample consists of 26 QSOs. Of these, the number of RQQs, LDQs, CDQs (the QSO 1512+370 was initially selected as a CDQ, but it is actually a LDQ; see SSGW03) and BLs are 7, 8, 6 and 5 respectively; in light of the relative paucity of BL Lacs, one object (1215+303) serves as a member of both Sets 1 and 2, and none was available in the highest redshift bin. The general properties of the objects monitored in this program are given in Table 1.

3 Radio observations and reductions

We wanted to include only those RQQs in our sample whose fluxes available are ≤ 1 mJy at 5 GHz. However, for two of the RQQs radio fluxes were not available in the literature. To ascertain the radio loudness of these two QSOs (1252+020 and 1029+329) in 1998 we carried out observations using the VLA¹. Snapshot observations at 5 GHz were made using the hybrid CnB configuration in a dual intermediate frequency mode with a total on-source integration time of 10 minutes. Maps of total intensity Stokes I were made from these data, using the CLEAN algorithm available in AIPS, attaining rms noise levels of $\sim 60 \mu\text{Jy}/\text{beam}$. They are displayed in Fig. 1. For objects with radio detection, measurement of the flux and position was carried out using the AIPS task JMFIT. A quasar is considered to have a positive detection when the radio source lies within $10''$ of the optical position. We detected the quasar 1252+020 at a level of 1 mJy whereas the quasar 1029+329 remained undetected down to a 0.2 mJy limit.

4 Optical observations and Data Reductions

4.1 Instrument

Observations of the quasars were carried out using the 104 cm Sampurnanand telescope of the State Observatory, Nainital. This is an RC system with a $f/13$ beam (Sagar 1999). The detector used for the observations was a cryogenically cooled 2048×2048 pixel² CCD, except prior to October 1999, when a smaller CCD of size 1024×1024 pixel² was used. In each CCD a pixel corresponds to a square of 0.38 arcsec size, covering a total sky area of about $12' \times 12'$ in the case of larger CCD and about $6' \times 6'$ in the case of smaller CCD. To increase the S/N ratio, observations were carried out in 2×2 binned mode. Practically all the observations were carried out using R filter, except on two nights, where quasi-simultaneous R and I filter observations were done. The choice of R filter in this observational program is because of it being at the maximum response of the CCD system; thus the time resolution achievable for each object is maximised.

¹The Very Large Array (VLA) of the National Radio Astronomy Observatory is operated by Associated Universities, Inc. under a cooperative agreement with the National Science Foundation

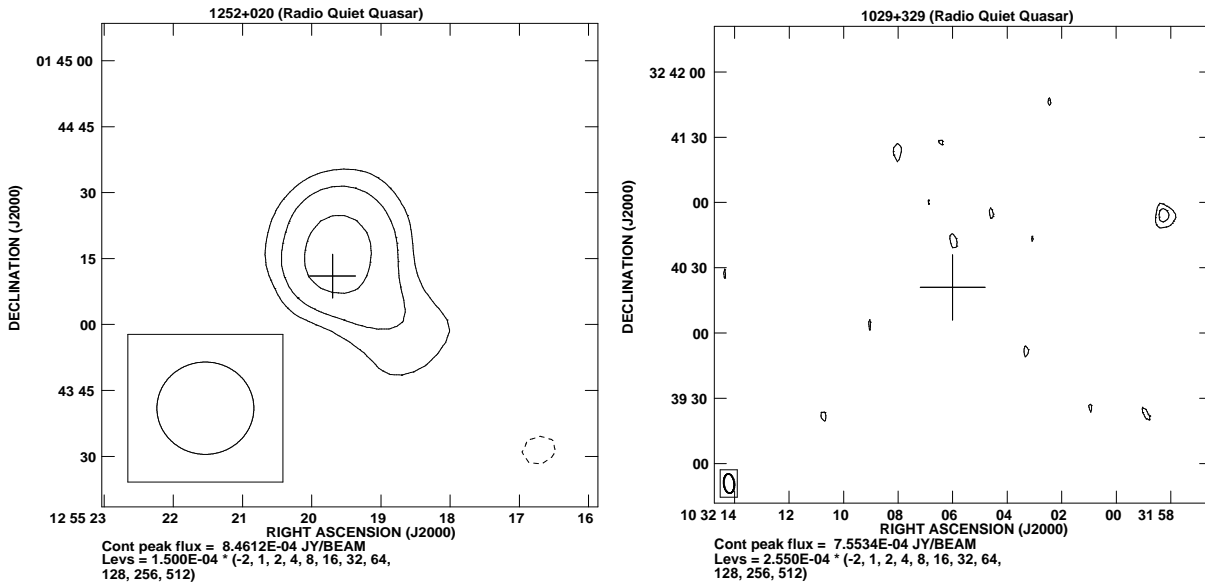


Figure 1. VLA 5 GHz image of the quasar 1252+020 (left) and 1029+329 (right).

4.2 Observing strategy

The goal of this observational program was to obtain temporally dense and sufficiently long duration data trains for each object, so that one could reliably detect statistically significant variations and determine the variability duty cycle (DC). Taking a clue from the optical monitoring of blazars, for which the probability of observing INOV in a given night is known to be greatly enhanced by continuous monitoring of at least 3 to 4 hours (Carini 1990), we have attempted to monitor each object for a minimum of 5 hours on each night. The typical time resolution is of the order of 10 minutes, which can allow ultra-rapid fluctuations to be picked up. However, on some nights time resolution is longer, ranging up to 30 minutes for the faintest objects in their weakest states.

Another important strategy adopted in this work is to sources and fields of view so as to ensure availability of suitable comparison stars. The position and apparent R magnitudes of the comparison stars used in the differential photometry of our sample of quasars are given in SGSW03 and SSGW03. Care was taken to have at least two, but usually more, comparison stars within 1 mag of the QSO on the CCD frame. This allowed us to identify and discount any comparison star which itself varied during a given night; this ensured reliable differential photometry of the QSO. Observations were made on a total of 113 for this programme during October 1998 – May 2002. A log of the observations, along with the results, are given in Table 2.

4.3 Data Reduction

Preliminary processing of the images as well as the photometry was done using the IRAF² software. The bias level of the CCD is determined from several bias frames (generally more than seven) taken intermittently during our observations over the night. A mean bias frame was formed using the task *zerocombine* in IRAF which was then subtracted from all the image frames of a night. Care was also taken in forming the mean bias frame such that they are not affected by cosmic-ray (CR) hits. The routine step of dark frame subtraction was not done as the CCDs used in the observations were cryogenically cooled to -120° C at which the rate of thermal charge is negligible for the exposure time of the present observations. Flat fielding was done by taking several twilight sky frames which were then median combined to generate the flat field template which was then used to derive the final frames. Finally CR hits seen in the flat fielded target frames were removed using the facilities available in MIDAS³.

4.4 Photometry

Aperture photometry on both the AGN and the comparison stars present on the flat-fielded CCD frames were carried out using the task *phot* in IRAF. A critical input to be specified to *phot* was the radius of the aperture

²IRAF is distributed by the National Optical Astronomy Observatories, which is operated by the Association of Universities for Research in Astronomy, Inc. under co-operative agreement with the National Science Foundation

³MIDAS stands for Munich Image and Data Analysis System and has been designed and developed by the European Southern Observatory (ESO) in Munich, Germany

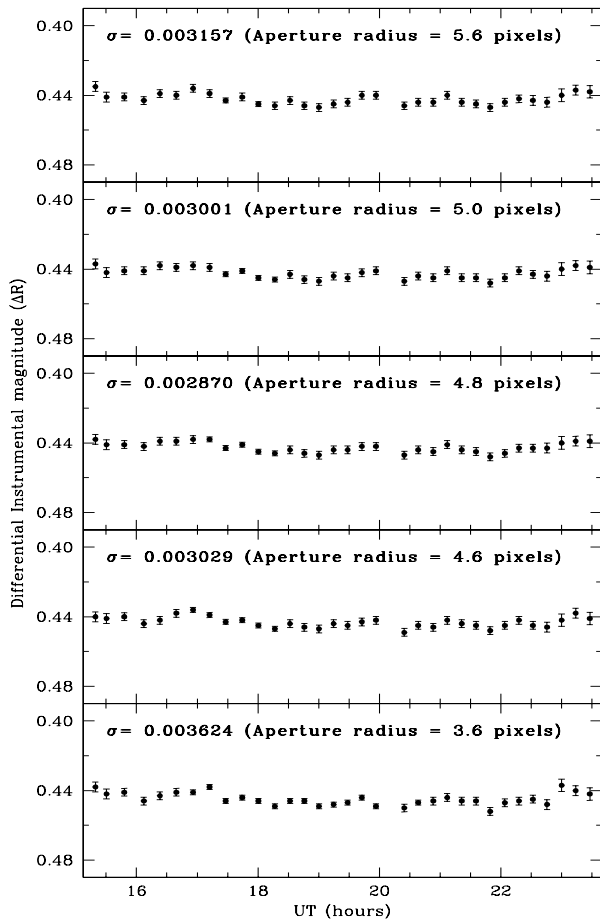


Figure 2. DLCs involving stars S2 and S3 in the field of the RQQ 1017+279 observed on 27 February 2000, for five different aperture radii showing the selection of optimum aperture. The minimum scatter occurs at an aperture radius of 4.8 pixels.

to perform the photometry. The selection of this aperture determines the S/N for each object in the frame. In an investigation by Howell (1989) the issue of an optimum aperture to maximize the S/N was discussed; this optimum aperture is found close to the FWHM of the PSF of the stars on the frame. By choosing an aperture that is close to the FWHM of a source, clearly some of the total flux from the source will be left out of the aperture. However, in this work only magnitude differences are important and not the absolute fluxes. Hence, this procedure of selecting an optimum aperture was promising for enhancing the photometric precision of the observations, since the S/N was maximised. The procedure we followed for finding an optimum aperture was identical to that used in Noble (1995). We specified several aperture radii (starting from the median FWHM of the night and incremented by 0.2 pixels) and then identified the aperture that yielded magnitudes of stars such that the scatter or variance of the resulting steadiest pair of Star – Star differential light curves (DLCs) was minimum. This process of finding the optimum aperture is illustrated in Fig. 1 which shows five DLCs for the same pair of comparison stars in the field of the quasar 1017+279 observed on 14 January 2000. The large variance at small apertures is due to the inclusion of fewer source pixels, whereas the large variance at large apertures is due to too many noise pixels compared to source pixels.

5 Potential sources of spurious intensity variations

5.1 Variable seeing

A potential source of spurious variability in aperture photometry is the contamination arising from the host galaxy of the AGN recorded in the CCD frame. This is because the surface brightness profile of any underlying galaxy will not respond to atmospheric seeing fluctuations in a manner similar to the central AGN. Thus intra-night fluctuations in the seeing could result in the variable contribution from the host galaxy within the aperture,

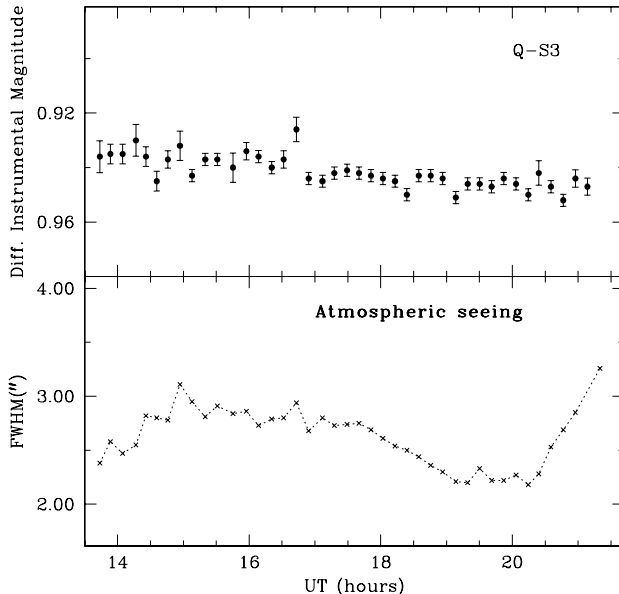


Figure 3. DLC of the LDQ 2349–014 observed on 17 October 2001 (top) and the variation of seeing during that night (bottom panel). The aperture radius used for the photometry is 5".

producing spurious changes in the brightness that could be mistaken for AGN variability. Recently the effect of spurious variations introduced in the DLCs by atmospheric seeing fluctuations has been quantitatively addressed by Cellone, Romero & Combi (2000). These authors conclude that spurious differential magnitude variations due to seeing fluctuation can be substantial for AGN with brighter hosts, particularly when small photometric apertures are used. However, our data are very unlikely to be affected by this, since all the quasars in our sample are very luminous ($M_B < -24.3$ mag) so that the nucleus is highly dominant *vis-à-vis* the host galaxy. In fact, the underlying host galaxy is not seen in any CCD images of our quasars except one, (LDQ 2349–014) which belongs to the lowest-redshift bin of our sample. Fig. 3 shows the DLC of this quasar relative to Star 3 together with the variation of atmospheric seeing during our observing night. The lack of any clear correlation between the quasar DLC and the seeing variations eliminates the possibility that the steady, slow decline seen in the quasar DLC is an artefact arising from seeing fluctuations. The FWHM in our whole observing program was generally between 1.4 and 4.4 arcsec.

5.2 Effects of colours of the comparison stars

Even on the clearest nights, objects are dimmed due to extinction by the Earth’s atmosphere. The amount of dimming depends on the airmass, the wavelength of observation and the prevailing atmospheric conditions. The observed magnitude (m_λ) is related to the magnitude above the Earth atmosphere (m_{λ_o}) as (Henden & Kaitchuck 1982)

$$m_\lambda = m_{\lambda_o} + (K'_\lambda + K''_\lambda c)X, \quad (1)$$

where K'_λ and K''_λ are respectively the principal and second order extinction coefficients, c is the colour index of the observed object and X is the airmass in the direction of the object. An advantage of performing differential photometry between the target and comparison stars located on the same CCD frame is that first order extinction effects on the differential magnitude cancels out, as both the comparison stars and the target are seen through nearly identical atmospheric layers making the same X . However, K''_λ which applies to the colour of the object can affect the differential magnitude. From Eq. (1) the differential magnitude between two objects of colour indices c_1 and c_2 is given by

$$\Delta m_\lambda = \Delta m_{\lambda_o} + K''_\lambda X \Delta c, \quad (2)$$

where $\Delta c = c_1 - c_2$, is the difference between the observed colour indices of the two objects. The relation between the standard and observed colour differences between the two objects can be written as

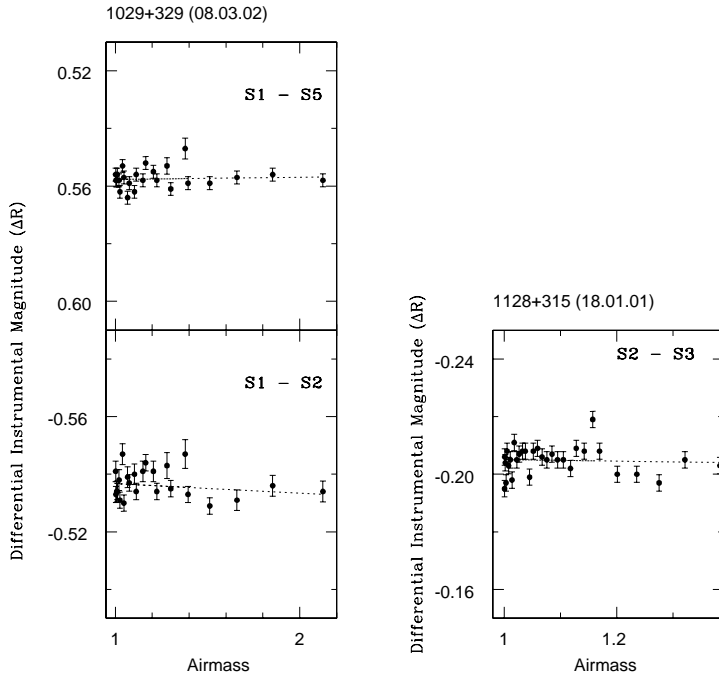


Figure 4. DLCs of the comparison stars in the field of 1029+329 (left panel) and 1128+315 (right panel) versus airmass.

Figure 5. Differential R-band lightcurves of radio-quiet quasars. The name of the object, the date and duration of observations are given on the top of each panel. The objects being compared and their colour differences (in parentheses) label the right side of each sub-panel.

$$\Delta C = \mu \Delta c, \quad (3)$$

where $\Delta C = C1 - C2$, is the difference between the standard colour indices of the two objects. As μ is close to unity (see Henden & Kaitchuck 1982) the observed colour index difference is not too different from the standard colour index difference. The values of $\Delta(B - R)$ between any quasar and comparison stars in our sample range between 0.4 and -2.5 mag. In order to investigate the effects of these colour differences on the DLCs of the quasars under study, the following analyses have been carried out.

From linear least square fitting of Eq. (2) using the standard colour index ($B-R$) taken from the United States Naval Observatory (USNO)⁴ catalog to the observations we found that the effect of second-order extinction is virtually negligible. To illustrate the effect of colour differences between the objects on their observed DLCs, we have shown in Fig. 4 (top panel) the observed instrumental magnitude difference between the stars S1 and S5 plotted against the airmass, whereas the bottom panel shows the magnitude difference between S1 and S2 plotted against the airmass. This is for the observations of the source 1029+329 carried out on the night of 8 March 2002 upto a maximum hour angle of 5 hour corresponding to $X \simeq 2.2$. Observations on other objects in our sample were also carried out on similar airmass at most. The colour difference $\Delta(B-R)$ between S1 and S2 is 1.9 while between S1 and S5 it is 0.9. From Fig. 4 (left panel) it is seen that despite a rather large range in airmass and a fairly large colour difference between the two stars, no artificial/spurious variations are introduced. Least square fits to both data sets shown in the left panel of Fig. 4 yields slopes of -0.0008 ± 0.0023 and 0.0033 ± 0.0037 , which are essentially zero. Also shown in Fig. 4 (right panel) is the observed instrumental magnitude difference between stars S2 and S3, having a difference in colour index of -1.4 , in the field of the QSO 1128+315 as observed on 18 January 2001. Linear regression analysis yield a slope of 0.0026 ± 0.0089 , which is again indistinguishable from zero. This effect is thus less than the photometric error of individual data points on the DLC and so we conclude that the colour differences between our sets of quasars and the comparison stars used in the differential photometry will not have any significant effects in the DLCs. Similar conclusions were also drawn by Carini et al. (1992) in their study of rapid variability of blazars.

⁴<http://archive.eso.org/skycat/servers/usnoa>

Figure 5. *continued*

Figure 5. *continued*

5.3 Error estimation of the data points in the DLCs

Determination of the basic variability parameters, such as peak-to-peak variability amplitudes, requires a realistic estimate of the photometric errors on individual data points of a given DLC. It has been argued recently in the literature that the photometric errors given by the reduction routines in IRAF and DAOPHOT underestimate the true errors. Considering the difference between the magnitudes of the added and recovered stars using the *addstar* routine of DAOPHOT, Gopal-Krishna et al. (1995) found that the formal errors returned by DAOPHOT are too small by a factor of 1.75. Similarly, Garcia et al. (1999) found that the error given by the *phot* task in IRAF is underestimated by a median factor of 1.73. In this work we have made an independent estimate of this systematic error factor. To do this we have considered those 108 nights of observations (out of the total 113 nights) which we have found useful for INOV studies. Out of these, we have identified 74 DLCs pertaining to ‘well behaved’ (i.e., stable) comparison stars. Only the best available star–star DLC for each of these nights were considered. The unweighted mean of a DLC consisting of N data points having amplitude X_i , is given by

$$\langle X \rangle = \frac{1}{N} \sum_{i=1}^N X_i, \quad (4)$$

and the variance of the DLC is

$$S^2 = \frac{1}{N-1} \sum_{i=1}^N (X_i - \langle X \rangle)^2. \quad (5)$$

Both intrinsic source variability and measurement uncertainty contribute to this observed variance. Under the assumption that both components are normally distributed and combine in quadrature the observed variance can be written as (see Edelson et al. 2002)

$$S^2 = \langle X \rangle^2 \sigma_{XS}^2 + \langle \sigma_{err}^2 \rangle. \quad (6)$$

The first term on the right represents the intrinsic scatter induced by source variability, and the second term is the contribution of measurement noise as returned by the *phot* task in IRAF. Assuming that the scatter of the data points is predominantly due to statistical uncertainty in the measurements, we have

$$\langle \sigma_{err}^2 \rangle = \frac{1}{N} \sum_{i=1}^N \sigma_{err,i}^2. \quad (7)$$

As we have considered here only star–star DLCs, the contribution of source variability to the observed variance S^2 may be taken to be zero and therefore S^2 becomes equal to the average of the squares of the measurement errors $\langle \sigma_{err}^2 \rangle$.

For each DLC we computed the quantity

$$Q = S^2 - \eta^2 \langle \sigma_{err}^2 \rangle, \quad (8)$$

where η^2 is the factor by which the average of the squares of the measurement errors should be incremented. For various assumed values of η we calculated the average of Q for the entire set of the 74 DLCs, as well as the numbers of DLCs for which Q was found to be positive and negative, respectively. The condition of the expectation value of Q being equal to zero (i.e. $\langle Q \rangle = 0$), is satisfied for $\eta = 1.55$. On the other hand, the median value of Q is zero for $\eta = 1.40$. Thus, we adopt a value of $\eta = 1.50$ in further analysis. Note that this value is somewhat lower than 1.75 estimated in Gopal-Krishna et al. (1995) and the 1.73 reported by Garcia et al. (1999).

6 Optical variability

In spite of the extensive observations (185.2 hours during 29 nights) of the 7 RQQs, optical variability was detected in only 3 objects during 28.1 hours on 5 nights. Similarly, out of 8 LDQs monitored on 37 nights during 271.2 hours of observations, only 4 showed optical variability during 57.1 hours of 9 nights. Of the 6 CDQs, only 3 showed optical variability during 43.2 hours of 5 nights out of 131.2 hours of monitoring during

20 nights. In contrast to them, all the 5 BL Lacs showed optical variability at some times during 110.8 hours of observations on 16 nights out of the monitored 148 hours during 22 nights. Thus, amongst the four classes of powerful AGNs BL Lacs are found to show maximum variability. In order to quantify these results, we have carried out the following analysis; below we discuss INOV and long-term optical variability (LTOV) separately.

6.1 Intra-night optical variability (INOV)

In total we have carried out 113 nights of observations, however, for INOV only 108 nights were considered, as the remaining 5 nights were too noisy to ascertain any variability (see Table 2). For blazars (CDQs and BL Lacs) our observations covered a total of 42 nights with an average of 6.6 hours/night (SSGW03). On the other hand for RQQs and LDQs our monitoring covered a total of 66 nights with an average of 6.1 hours/night (SGSW03). Out of the total of 108 observing epochs, nightly DLCs for 10 LDQs, 8 RQQs and 1 BL Lac and CDQ each are presented in SGSW03, while the DLCs of another 24 nights (16 BL Lacs, 6 CDQs & 2 LDQs) are presented by SSGW03. In this paper we present the INOV DLCs for the remaining 64 nights of observation in Figs. 5, 6, 7 and 8 for RQQs (21 nights), LDQs (22 nights), CDQs (16 nights), and BL Lacs (5 nights), respectively. This program has led to the first clear detection of INOV in RQQs (see GSSW03). A clear distinction between the INOV nature of the two classes of relativistically beamed radio-loud AGNs (CDQs and BL Lacs) is found for the first time (SSGW03).

The variability nature of an AGN on a given night of observation is ascertained following a statistical criterion based on the parameter C_{eff} , which is similar to the parameter C used by Jang & Miller (1997), with the added advantage that for each AGN we have DLCs relative to multiple comparison stars. The details of C_{eff} determination are explained in SGSW03. We consider a quasar to be variable if $C_{\text{eff}} > 2.57$, which corresponds to a confidence level of variability in excess of 99%. A quasar is classified as a probable variable (PV) if $2.57 \geq C_{\text{eff}} > 2.00$. The values of C_{eff} for variable and probable variable quasars along with the variability status of each of the quasars monitored in this program is given in Table 2.

We also calculated the variability amplitude of quasars which are found to be variable and probable variable. Following Romero et al. (1999), the amplitude of variability of a DLC is defined as

$$\psi = \sqrt{(D_{\text{max}} - D_{\text{min}})^2 - 2\sigma^2}, \quad (9)$$

where D_{max} , D_{min} are the maximum and minimum in the quasar differential lightcurve relative to a stable star and $\sigma^2 = \eta^2 \langle \sigma_{\text{err}}^2 \rangle$. We have found $\eta = 1.50$ (see Sect. 5.3). The calculated values of ψ for quasars showing INOV is given in Table 2.

6.1.1 Structure function analysis

Structure function analysis is a very useful pointer to the variability characteristics of the lightcurve. It manifests time-scales and periodicities present in the lightcurves. The general definition of structure functions (SFs) and some of their properties are described, e.g., by Simonetti et al. (1985), Heidt & Wagner (1996) and Hughes, Aller & Aller (1992). Following Simonetti et al. (1985) we have defined the first-order structure function as

$$D_X^1(\tau) = \frac{1}{N(\tau)} \sum_{i=1}^N [X(i+\tau) - X(i)]^2, \quad (10)$$

where τ = time lag, $N(\tau) = \sum w(i)w(i+\tau)$ and the weighting factor $w(i) = 1$ if a measurement exists for the i^{th} interval, and 0 otherwise.

The error in each point in the computed SF is

$$\sigma^2(\tau) = \frac{8\sigma_{\delta X}^2}{N(\tau)} D_X^1(\tau), \quad (11)$$

where $\sigma_{\delta X}^2$ is the measured noise variance.

Since the sampling of our DLC is quasi-uniform, we have determined the SF using an interpolation algorithm. For any time lag τ , the value of $X(i+\tau)$ was calculated by linear interpolation between the two adjacent data points. A typical time scale in the light curve (i.e., time between a maximum and a minimum, or vice versa) is indicated by a local maximum in the SF. In case of a monotonically increasing structure function, the source possesses no typical time-scale smaller than the total duration of observations. An indication of periodicity can be inferred from minima of the SF. The SF plots as well as their behaviour for 2 CDQs, 1 LDQ and 5 BL Lacs which showed definite INOV during 13 nights of observation are given in SSGW03. Here we present SF plots for 3 RQQs and 3 LDQs which confirmed INOV during 10 nights of observations in Figs. 9 and 10 respectively.

The inferred variability timescale(s) and “period”(s) are given in Table 2. Because none of our light curves were long enough to show more than two maxima or minima, it should be stressed that we are not claiming that we have detected actual periodic components of the INOV in any of our sources.

6.1.2 Duty cycles of intra-night optical variability (DC)

The high precision of our data permit the estimation of INOV duty cycle (DC) not only for different AGN classes, but also for different levels of variability amplitudes. The DC of INOV of a given class of objects is given by (Romero et al. 1999)

$$DC = 100 \frac{\sum_{i=1}^n N_i (1/\Delta t_i)}{\sum_{i=1}^N (1/\Delta t_i)} \quad \%, \quad (12)$$

where $\Delta t_i = \Delta t_{i,obs}(1+z)^{-1}$ is the duration (corrected for cosmological redshift) of a i^{th} monitoring session of the source in the selected class. N_i equals 0 or 1, depending on whether the object was respectively, non-variable, or variable during Δt_i .

A DC of 17% was found for RQQs considering only sessions for which INOV was unambiguously detected. This value is roughly midway between the lower values published by Jang & Miller (1997) and Romero et al. (1999) and the higher estimate of de Diego et al. (1998). For LDQs a DC of only 12% is found for clear detection of INOV; however, this rises to about 18% if the two cases of probable detection are included. Also, the range of DCs for both RQQs and LDQs are found to be very similar (see Table 2). This similarity between LDQs and RQQs in terms of INOV even extends to BL Lacs if small amplitudes ($\psi < 3\%$) variation is considered (GSSW03). Detailed explanations of the similarities in the INOV characteristics of RQQs and LDQs compared to BL Lacs are given by SSGW03. Also, a clear distinction is found in DCs between the two presumably relativistically beamed AGN classes, namely BL Lacs and CDQs. BL Lacs are found to show a high DC, $\sim 72\%$, whereas CDQs show a DC of about 20%. However, separating the CDQs into high polarization (CDQ-HP) and low polarization (CDQ-LP) subsets seems to be relevant; CDQ-LP show very low DC ($< 10\%$), whereas a much higher value of DC is found for the CDQ-HP sources (51%). It thus appears that INOV is more closely connected to high optical polarization than to Doppler boosting *per se*. Such polarized emission is commonly attributed to shocks in relativistic jets (see SSGW03 for details).

6.1.3 Relativistic beaming, Doppler factor and accretion efficiency

We have estimated the observed Doppler factor (δ_{obs}) and accretion efficiency (η_{obs}) in the framework of the relativistic beaming models (e.g., Marscher & Scott 1980). The apparent R magnitudes of the quasars (m_R) were obtained from their observed DLCs using the apparent R magnitudes of the comparison stars given in USNO catalog. These were converted to observed monochromatic fluxes (S_R) following Bessel (1979) as

$$S_R = 3.08 \times 10^{-23} 10^{-0.4m_R} \quad \text{W m}^{-2}\text{Hz}^{-1}. \quad (13)$$

The rest-frame observed monochromatic luminosity of the source at frequency ν_o (which we take as the frequency corresponding to the V-band)

$$L_{\nu_o} = 4\pi \left(\frac{cz}{H_o} \right)^2 \left(1 + \frac{z}{2} \right)^2 S_{\nu_o} \quad \text{for } q_o = 0, \quad (14)$$

where

$$S_{\nu_o} = S_{\nu_{obs}} \left[\frac{\nu_o}{\nu_{obs}(1+z)} \right]^\alpha (1+z)^{-1}, \quad (15)$$

and where ν_{obs} = frequency corresponding to R-band, $S_{\nu_{obs}}$ = flux observed in R-band, and $\alpha = d(\ln S)/d(\ln \nu)$.

The observed bolometric luminosity is then calculated from this monochromatic luminosity, using the scaling factor given by Elvis et al. (1994) for V-band as

$$L_{Bol}/L_V = 13.2, \quad (16)$$

where $L_V = \nu L_\nu$ at V-band ($\nu = 5.456 \times 10^{14}$ Hz) (Elvis et al. 1994).

We have defined Δt_{min} as the minimum variability time-scale observed for a clearly detected fluctuation on a given night, corrected to the intrinsic value in the source frame, by dividing Δt_{obs} with $(1+z)$.

Luminous outbursts of energy ΔL (ergs s^{-1}), cannot occur on time-scales, Δt_{min} , much shorter than the light crossing time of the emitting region. In this case, the inferred efficiency (η_{obs}) for the conversion of accreted

matter into energy for the case of spherical, homogeneous, non-relativistically beamed co-moving emitter is given as (Fabian & Rees 1979)

$$\eta_{obs} \geq 5 \times 10^{-43} \Delta L / \Delta t_{min}. \quad (17)$$

Assuming that the bolometric luminosity also changes in the same manner as does the flux during outburst (e.g., Zhang, Fan & Cheng 2002), we have estimated η_{obs} , taking ΔL to be the variable fraction of the bolometric luminosity during Δt_{min} .

It is known that the efficiency of energy production in the nuclear reaction is 0.007 and that for disk accretion, the value of η_{int} is smaller than ~ 0.3 for rapidly rotating black holes (e.g. Frank, King & Raine 1986). We have calculated the lower limit of η_{obs} for all the quasars in our sample which show definite variability and the results are given in Table 2. If η_{obs} is found to be greater than 0.1, relativistic beaming is usually invoked to explain the observations.

Once η_{obs} is known, one can calculate δ_{obs} . Since $\Delta L(obs) = \delta_{obs}^{3+\alpha} \Delta L(int)$ and $\Delta t_{min}(obs) = \delta_{obs}^{-1} \Delta t_{min}(int)$ (Worrall 1986; Frank, King & Raine 1986); if we let $\eta_{obs} = 5 \times 10^{-43} \Delta L(obs) / \Delta t_{min}(obs)$, We then find $\eta_{int} = 5 \times 10^{-43} \Delta L(int) / \Delta t_{min}(int)$, and thus

$$\delta_{obs} \geq (\eta_{obs} / \eta_{int})^{1/(4-\alpha)}. \quad (18)$$

If η_{int} is known, δ_{obs} can now be calculated. Given that that η_{int} has a range from 0.007 for nuclear reaction to 0.32 for maximal accretion, we choose a geometric mean for η_{int} of ~ 0.05 , which is almost equal to the value of 0.057 derived from non-rotating accretion disk theory (e.g., Paczyński & Wiita 1980) in estimating δ . The derived (δ_{obs}) for all the variable objects with $\eta_{obs} \geq 0.1$ in our sample are given in Table 2. The average and median values of η_{obs} are 0.89 and 0.33 respectively, while δ_{obs} range between 1 to 2.55 with a mean and median of 1.6 and 1.6 respectively.

6.2 Long term optical variability (LTOV)

Long term optical variability (LTOV) is seen in 20 out of 26 objects in our sample during the period of our observations. The number of epochs covered range between three and seven and the total time span covered range between about a week to three years. The LTOV light curves for 11 quasars (6 CDQs and 5 BLs) are given by SSGW03, while the same for another 3 quasars (2 LDQs and 1 RQQ) are presented by SGSW03. Here we present the LTOV light curves of the remaining 12 objects in our sample and comment on those individual sources in increasing order of redshift.

LDQ 2349–014, $z = 0.174$: This QSO was monitored for three epochs which covered a time baseline of only five days. Over this time span the QSO was found to vary significantly. It faded by about 0.03 mag over four days between 13 October 2001 and 17 October 2001 and within the next 24 hours it brightened by about 0.05 mag (Fig. 11).

RQQ 0945+438, $z = 0.226$. This object was observed on three epochs and time baseline extends over nearly three years. As neither of the comparison stars remained stable between our first epoch and the subsequent two epochs, we have considered only the latter two epochs 26 February 2000 and 23 January 2001 to examine the LTOV. The quasar dimmed by 0.07 mag within about a year between the two epochs (Fig. 12)

RQQ 0514–005, $z = 0.291$. Our three epochs of observations on this quasar covered a time baseline of about 10 days. The QSO did not show any change in brightness in about 24 hours during the first two epochs, but it faded by about 0.01 mag between 10 December 2001 and 19 December 2001 (Fig. 12).

RQQ 1252+020, $z = 0.345$: This QSO was monitored for five epochs; however, for LTOV only four epochs could be considered as the first epoch (22 March 1999) lacks common comparison stars with the later four epochs. The total time baseline covered was about 2 years. The quasar remained at the same brightness level during the first two epochs of observations (9 March 2000 and 3 April 2000). It brightened by about 0.18 mag when observed a year later on 26 April 2001. Observations on 18 March 2002 showed the object to have dimmed by about 0.10 mag compared to 26 April 2001 (Fig. 12).

LDQ 0134+329, $z = 0.367$: Three nights of observations were taken on this object, but they cover a time baseline of just six days. The object remained at the same brightness level during the first two days (7 November 2001 and 8 November 2001), but dimmed by about 0.02 mag when observed again on 13 November 2001 (Fig. 11)

RQQ 1101+319, $z = 0.440$: Both brightening and fading were clearly present in our four epochs of observations which cover a time baseline of about two years. A fading of about 0.19 mag was noticed in a year between the first two epochs of observations (12 March 1999 and 4 April 2000). When observed a year later (21 April 2001) a reversal in this trend was noticed whereby the quasar brightened by about 0.006 mag and thereafter remained steady during the next 24 hours (Fig. 12).

LDQ 0709+37, $z = 0.487$: The LTOV nature of this QSO can be gleaned from the five epochs of observations done in the year 2001. It remained at the same brightness level during the first three epochs of observations

during January 2001. However, it brightened by about 0.03 mag when observed on 20 December 2001 and then faded by about 0.09 mag within the next 24 hours (between 20 and 21 December 2001; see Fig. 11).

RQQ 1029+329, $z = 0.560$: This QSO was monitored on six nights; however, for characterizing the LTOV only the later five epochs were considered due to the lack of common comparison stars in the first epoch of observation. The QSO remained at the same brightness level during our last five epochs of observations (between 2 March 2000 and 8 March 2002) covering a two year baseline (Fig. 12)

LDQ 0350-073, $z = 0.962$: The quasar was found not to show any variability during our three epochs of observations within a week (during 14 to 18 November 2001) (Fig. 11).

LDQ 0012+305, $z = 1.619$. The quasar was found to be variable from our six epochs of observations encompassing about 10 months during 2001. It remained at the same brightness level during the first three epochs of observations and then faded by about 0.06 mag when observed nine months later on 14 October 2001. It then remained at the same brightness level for the next one week during which it was monitored on three nights (Fig. 11)

RQQ 1017+279, $z = 1.918$. This quasar was monitored on three epochs. However, its LTOV could only be probed from the later two epochs, due to the lack of common comparison stars between them and the first epoch. The quasar remained at the same flux level between the last two epochs (i.e., 14 January 2000 and 27 February 2000) separated by seven weeks (Fig. 12)

CDQ 1225+317, $z = 2.219$. No evidence of variability is found over the 2 year time (between March 1999 and April 2001) covered by our three epochs of observations (Fig. 11).

7 Do INOV and LTOV have a common origin?

A perception has gradually been developed that the most common cause of rapid optical variability of blazars is associated with disturbance occurring within their relativistic jets. For instance, Romero et al. (1999) have argued that while the LTOV arises due to large-scale relativistic shocks propagating through the jet, the INOV occurs due to the interception of these shocks by small scale magnetic irregularities in the jet. To verify these ideas, one needs to have a really large database of INOV monitoring observations at multiple epochs. Nonetheless, our fairly extensive database allows us to perform a check by searching for a correlation between the INOV amplitude and the level of optical brightness of the quasar. To do this, we have considered a subset of 5 ‘blazars’ in our sample, for which INOV was clearly detected on at least two nights. The LTOV information was obtained from our multi-epoch data. This was done by further identifying at least one stable (‘well behaved’) comparison star common to all the epochs and then calculating the mean optical magnitude of the quasar relative to that star for each epoch. The night for which the quasar had the minimum optical brightness is taken as the base level for LTOV and the resulting offset values of the quasars magnitudes are given in Table 3, in the sequence of increasing brightness. Thus, these data provide a decent quantitative description of the LTOV of the quasars. It may, however, be noted that due to the scheduling constraints, the total time span covered is highly variable from quasar to quasar, as can be seen from our log of observations in Table 2.

Fig. 13 shows the comparison of LTOV and INOV amplitudes for the subset of 5 blazars and one LDQ following the prescription above. Different symbols are used for each object and the multi-epoch data for a given object are joined by dashed lines. It is fair to state that, based on our dataset, no unambiguous general trend for a correlation between the INOV and LTOV amplitudes is evident for these luminous AGNs. Thus, from an observational point of view, there is as yet no strong case for assuming common excitation conditions for LTOV and INOV in the optical output of blazars.

7.1 Do accretion disks contribute to INOV?

The relation of INOV to the long term variability nature of quasars can be used to ascertain the contribution of disk emission to INOV (e.g., Mangalam & Wiita 1993). Several Optically Violent Variables (OVVs) including 3C 345 (Bregman et al. 1986; Smith et al. 1986), PKS 0420-014, B2 1156+295 and 3C 454.3 (Smith et al. 1988) supply photometric and polarimetric evidence for substantial accretion disk contributions to their emission. But the general absence of a Big Blue Bump in BL Lac spectra does not provide the strong evidence in favour of an accretion disk components that exists in most quasars (Sun & Malkan 1989). Still it has been claimed that in one of the best studied BL Lacs, 2155-304, an accretion disk does seem to contribute to their spectrum (Wandel & Urry 1991). However, optical polarimetry of the source implies that the disk contribution, if present, is fairly small (Smith & Sitko 1991).

If INOV is found to be inversely correlated to the brightness state of the object this may provide evidence for the accretion disk contribution to the observed INOV. This is because the disk component will be relatively more important when the object is in a quiescent state and jets are weaker. A comparison of INOV against

LTOV for all the BL Lacs in our sample is shown in Fig. 13. No correlation between INOV and LTOV is noticed suggesting little contribution of an accretion disk to the observed INOV in any of these sources.

7.2 INOV in the context of the starburst models of AGN

In the starburst model (Terlevich et al. 1992; Terlevich & Melnick 1985) of AGNs, variability results from random superposition of events such as supernova explosions generating rapidly evolving compact supernova remnants (cSNRs) due to the interaction of their ejecta with the high density circumstellar environment. This model is supported by the striking similarity between the optical spectra of some AGNs and of cSNRs (Filippenko et al. 1989). The characteristics of an event (i.e., light curve, amplitude and time-scale) results from the combination of complicated processes (Terlevich et al. 1992). Still, the lightcurves of AGNs of various absolute luminosities and redshifts can be predicted from the model and are found to be reasonably consistent with the observed dependence of structure function (the curve of growth of variability with time) on luminosity and redshift (cid Fernandes, Aretxaga & Terlevich 1996; Cristiani et al. 1996). The lightcurves of cSNRs are still poorly known. While they seem to be consistent with the optical lightcurves of the low luminosity AGNs, NGC 4151 and NGC 5548 (Aretxaga & Terlevich 1994), as argued by cid Fernandes, Aretxaga & Terlevich (1997) and references therein, starburst models may be useful in explaining variability of modest amplitude in very weak AGN ($M_B \sim -20$ is the peak of a cSNR). As the energies involved in the intra-night fluctuations we have detected are at least an order of magnitude above these, it appears that such a model has negligible applicability to the variability events associated even with the non-blazar type AGNs (Tables 2 and 3).

7.3 INOV and polarization: instances of exceptional behaviour

High and variable optical polarization is one of the defining characteristics of blazars (Angel & Stockman 1980) whose radiation is now believed to be dominated by relativistically boosted non-thermal jet emission (Blandford & Rees 1978). To investigate the relationship of optical INOV to the polarization, we have plotted the duty cycles of the 10 variable quasars in our sample against their optical polarizations (Fig. 14). It is found that the INOV is seen more in high polarization quasars ($P_{opt} > 3\%$). The main exception in our sample is, curiously, the BL Lac object 0735+178 for which a very high degree of optical polarization ($P_{opt} = 14.1\%$) has been reported (Table 1). Moreover, a CDQ, 1308+326, even though highly polarized ($P_{opt} = 10.2\%$) has shown INOV on just one of the five nights on which it was monitored (for 6 to 8 hours duration each time). However, in this case, the non-detection of INOV on four of the nights could well be the result of the blazar being too faint, leading to abnormally noisy DLCs which would mask more typical variations. In contrast, an exceptionally noteworthy case is the LDQ 2349–014 which is very weakly polarized ($P_{opt} = 0.91\%$) and yet showed INOV on all the three nights it was monitored. However its INOV is of low level ($\psi < 3\%$) and may even be the part of a longer time-scale variation. The weak correlation visible in Fig. 14, along with our results of the DC of INOV discussed above (Sect. 6.1.2) argues that INOV is closely associated with optical polarization.

8 Conclusions

In this extensive optical monitoring programme, an effort has been made to understand the INOV characteristics of the four major classes of luminous AGNs, namely radio-quiet quasars, radio-lobe dominated quasar, radio-core dominated quasars and BL Lac objects. The major finding of this present study are:

1. The first clear evidence of INOV in RQQs has been found from this observational programme (Gopal-Krishna et al. 2003).
2. BL Lac objects are found to show high DC of INOV (72%). In contrast, LDQs, CDQs and RQQs show much smaller INOV duty cycles ($\sim 20\%$). Although our estimate of the DC of RQQs is much higher than 3% found by Romero et al. (1999), it clearly falls much short of the DC for BL Lacs. In this sense, there is still a marked difference between the INOV properties of radio-loud and radio-quiet quasars, in contrast to the conclusions reached by de Diego et al. (1998), namely that INOV occurs as frequently in RQQs as it does in RLQs. This different conclusion of ours is probably due to our higher sensitivity, and the distinctly temporally denser monitoring achieved in our program.
3. The high DC shown by BL Lacs strongly suggests that relativistic beaming plays an important role in their observed micro-variability. Nonetheless, the lower DC and amplitude of INOV, shown by LDQs and RQQs can be understood within the framework of unified models, as these objects are believed to have modestly misaligned jets (see GSSW03). We infer that LDQs and even RQQs could possess relativistic, optical synchrotron nuclear jets on micro-arcsecond scales. Their intrinsic variability can thus be similar

to BL Lacs, and their observed much milder INOV can be attributed to their (micro) jets being modestly misaligned from our direction (and so having lower Doppler factors δ). Thus, the observed difference in the micro-variability nature of LDQs and RQQs compared to BL Lacs can be accounted for in terms of their optically emitting nuclear jets undergoing different degrees of Doppler boosting in our direction. Observers located in suitably different directions may well find these same LDQs and RQQs to be large-amplitude rapid variables (GSSW03).

4. For blazars, no correlation is noticed between their INOV amplitude and their apparent optical brightness (Fig. 13). This suggests that the physical mechanisms of intra-night and long-term optical variability do not have one-to-one relationship, and other factors are involved. Likewise, the absence of a clear negative correlation between the INOV and LTOV characteristics of the blazars in our sample points towards an inconspicuous contribution of accretion disk to the observed INOV, though we stress that our sample size is very small and no firm conclusions can yet be drawn.
5. A clear distinction is found for the first time between the INOV properties of the two classes of relativistically beamed radio-loud AGNs (RLQs), namely, BL Lacs and CDQs. The latter are found to exhibit low INOV duty cycle, no more than that exhibited by RQQs and LDQs. Moreover BL Lacs show high amplitude and DC of INOV. But in confining the discussion only to the CDQs which have high optical polarization, it is found that they resemble BL Lacs, both in amplitude and DC of INOV. It thus appears that the mere presence of a prominent (and hence Doppler boosted) radio core does not guarantee INOV; rather it appears that the more crucial factor is the optical polarization of the core emission. Such polarized emission is normally associated with shocks in a relativistic jet. This strongly suggests that the INOV is associated predominantly with highly polarized quasars (see SSGW03).
6. Even though the percentage luminosity variations implied by the INOV for these luminous AGNs is small, the total power involved is still so enormous so as to render a starburst/supernova explanation untenable for these rapid events.

Acknowledgments

The help rendered by the technical staff at the 104 cm telescope of State Observatory, Nainital is thankfully acknowledged. This research has made use of the NASA/IPAC Extragalactic Database (NED), which is operated by the Jet Propulsion Laboratory, California Institute of Technology, under contract with the National Aeronautics and Space Administration. CSS thanks NCRA for hospitality and use of its facilities. PJW's efforts were partially supported by Research Program Enhancement funds at GSU, and he is grateful for hospitality at Princeton University Observatory.

References

- [1] Angel J.R.P., Stockman H.S., 1980, *ARA&A*, 18, 321
- [2] Aretxaga I., Terlevich R., 1994, *MNRAS*, 269, 462
- [3] Bessel M.S., 1979, *PASP*, 91, 589
- [4] Berriman G., Schmidt G.D., West S.C., Stockman H.S., 1990, *ApJS*, 74, 869
- [5] Blandford R.J., 2000, *Trans. Roy. Soc. A* (astro-ph/0001499)
- [6] Blandford R.J., Rees M.J., 1978, in *Pittsburgh Conference on BL Lac Objects*, ed. A. Wolfe (U. Pittsburgh) p. 328
- [7] Blundell K.M., Beasley A.J., 1998, *MNRAS*, 299, 165
- [8] Blundell K.M., Rawlings S., 2001, *ApJL*, 562, L5
- [9] Boyle B.J., Shanks T., Croom S.M., Smith R.J., Miller L., et al. 2000, *MNRAS*, 317, 1014
- [10] Bregman J.N., Glassgold A.E., Huggins P.J., Kinney A.L., 1986, 301, 708
- [11] Carini M.T., 1990, Ph.D. thesis, Georgia State University, Atlanta, USA
- [12] Carini M.T., Miller H.R., Noble J.C., Goodrich B.D., 1992, *AJ*, 104, 15

- [13] Cellone S.A., Romero G.E., Combi J.A., 2000, AJ, 119, 1534
- [14] Cirasuolo M., Magliocchetti A., Celloti A., Danese L., 2003 (astro-ph/0301526)
- [15] Cristiani S., Trentini S., La Franca F., Aretxaga I., Andreani P., Vio R., Gemmo A., 1996, A&A, 306, 395
- [16] de Diego J.A., Dultzin-Hacyan D., Ramirez A., Benitez E. 1998, ApJ, 501, 69
- [17] Dunlop J.S., McLure R.J., Kukula M.J., Baum S.A., O’Dea C.P., Hughes D.H., 2003 (astro-ph/0108397)
- [18] Edelson R.A., Turner T.J., Pounds K., Vaughan S. et al. 2002, ApJ, 568, 610
- [19] Elvis M., Wilkes B.J., McDowell J.C., Green R.F., Bechtold J., Willner S.P., Oey M.S., Polomski E., Curti R., 1994, ApJS, 95, 1
- [20] Fabian A.C., Rees M.J., 1979, in X-ray Astronomy (eds) W. A. Barty and L.E. Peterson p, 381
- [21] Falcke H., Patnaik A.R., Sherwood W., 1996, ApJ, 473, L13
- [22] Fernandes C. R., Terlevich R., Aretxaga I., 1997, MNRAS, 289, 318
- [23] Fernandes C. R., Aretxaga I, Terlevich R., 1996, MNRAS, 282, 1191
- [24] Filippenko A. V., 1989, AJ, 97, 726
- [25] Frank J., King A.R., Raine D.J., 1986, Accretion Power in Astrophysics (Cambridge University Press, Cambridge)
- [26] Garcia A., Sodre L., Jablonski F.J., Terlevich R.J., 1999, MNRAS, 309, 803
- [27] Goldschmidt, P., Kukula, M.J., Miller, L., Dunlop, J.S., 1999, ApJ, 511, 612
- [28] Gopal-Krishna, Sagar R., Wiita P.J., 1995, MNRAS, 274, 701
- [29] Gopal-Krishna, Gupta A.C., Sagar R., Wiita P.J., Chaubey U.S., Stalin C.S. 2000, MNRAS, 314, 888
- [30] Gopal-Krishna, Stalin C. S., Sagar R., Wiita P. J., 2003, ApJ, 586, L25 (GSSW03)
- [31] Ho L.C., 2002, ApJ, 564, 120
- [32] Heidt J., Wagner S. J., 1996, A&A, 305, 42
- [33] Henden A., Kaitchuck 1982, in Astronomical Photometry
- [34] Howell S. B., 1989, PASP, 101, 616
- [35] Hughes P.A., Aller A.D., Aller M.F., 1992, ApJ, 396, 469
- [36] Hutsemekers D., Lamy H., 2001, A&A, 367, 381
- [37] Ivezić Z. et al., 2002, AJ, 124, 2364
- [38] Jang M., Miller H.R. 1995, ApJ, 452, 582
- [39] Jang M., Miller H.R. 1997, AJ, 114, 565
- [40] Kellermann K.I., Sramek R., Schmidt M., Shaffer D.B., Green R., 1989, AJ, 98, 1195
- [41] Kellermann K.I., Sramek R.A., Schmidt M., Green R.F., Shaffer D.B., 1994, AJ, 108, 1163
- [42] Kukula M.J., Dunlop J.S., Hughes D.H., Rawlings S., 1998, MNRAS, 297, 366
- [43] Kundt W., 2002, New Astronomy Reviews, 46, 257
- [44] Marscher A. P., Gear W. K., 1985, ApJ, 298, 114
- [45] Marscher A., Scott J.S., 1980, PASP, 92, 127
- [46] Marscher A. P., Gear W. K., Travis J. P., 1992, in Variability of Blazars, eds. Valtaoja E., Valtonen M. (Cambridge Univ. Press, Cambridge) p. 85

- [47] Mangalam A. V., Wiita P. J., 1993, *ApJ*, 406, 420
- [48] McLure R.J., Dunlop J., 2001 in *QSO hosts and their environments*, eds., Marquez I. et al. (Kluwer, Dordrecht) p. 27
- [49] Meier D.L., 2002, *New Astronomy Reviews*, 46, 247
- [50] Miller P., Rawlings S., Saunders R., 1993, *MNRAS*, 263, 425
- [51] Miller H. R., Carini M. T., Goodrich B. D., 1989, *Nature*, 337, 627
- [52] Noble J.C., 1995, Ph.D. thesis, Georgia State University, Atlanta, USA
- [53] Paczyński B., Wiita P.J., 1980, *A&A*, 88, 23
- [54] Papadopoulos P.P., Seaquist E.R., Wrobel J.M., Binette L., 1995, *ApJ*, 446, 150
- [55] Rabbette M., McBreen B., Smith N., Steel S. 1998, *A&AS*, 129, 445
- [56] Romero C.E., Cellone S.A., Combi J.A., 1999, *A&AS*, 135, 477
- [57] Sagar R., 1999, *Current Science*, 77, 643
- [58] Sagar R., C. S. Stalin, Gopal-Krishna, Wiita P.J., 2003 *MNRAS submitted* (SSGW03)
- [59] Schmidt M., Green R.F., 1983, *ApJ*, 269, 352
- [60] Simonetti J. H., Cordes J. M., Heeschen D. S., 1985, *ApJ*, 296, 46
- [61] Smith P.S., Sikto M.L., 1991, *ApJ*, 383, 580
- [62] Smith P.S., Balonek T.J., Heckert P.A., Elston R., 1986, *ApJ*, 305, 484
- [63] Smith A.G., Leacock R.J., Webb J.R., 1988, in *Variability in Active Galactic Nuclei*, eds., H.R. Miller, P. J. Wiita (Springer, Berlin) p. 158
- [64] Stalin C.S., Gopal-Krishna, Sagar R., Wiita P.J., 2003 *MNRAS submitted* (SGSW03)
- [65] Stocke T.J., Morris S.L., Weymann R.J., Foltz C.B., 1992, *ApJ*, 396, 487
- [66] Sun W.H., Malkan M.A., 1989, *ApJ*, 346, 68
- [67] Terlevich R., Melnick J., 1985, *MNRAS*, 213, 84
- [68] Terlevich R., Tenorio-Tagle G., Franco J., Melnick J., 1992, *MNRAS*, 255, 713
- [69] Veron-Cetty M.P., Veron P., 1998, *ESO Scientific Report No. 18*
- [70] Wandel A., Urry C.M., 1991, *ApJ*, 367, 78
- [71] White, R.L., et al., 2000, *ApJS*, 126, 133
- [72] Wills B.J., Wills D., Breger M., Antonucci R.R.J., Barvainis R., 1992, *ApJ*, 398, 454
- [73] Wilson A.S., Colbert E.J.M., 1995, *ApJ*, 438, 62
- [74] Wisotzki L., 2000, *A&A*, 353, 853
- [75] Wiita P. J., 1996, in *Blazar Continuum Variability*, eds., Miller H. R., Webb J. R., Noble J. C., *Astr. Soc. Pacific Conf. Ser. 110*, (ASP, San Francisco) p. 42
- [76] Woo J.M., Urry C. M., 2002, *ApJ*, 581, L5
- [77] Worrall D.M., 1986, *ApJ*, 303, 589
- [78] Zhang L.Z., Fan J.H., Cheng K.S., 2002, *PASJ*, 54, 159

Table 1: General information on radio-quiet, lobe-dominated, core-dominated and BL Lac objects monitored in the present programme. The quasar 1512+370 initially selected as a CDQ is actually a LDQ (see SSGW03)

Set No.	Object	Other Name	Type	RA(2000)	Dec(2000)	B (mag)	M_B (mag)	z	%Pol [†] (opt)	log R [‡]
1.	0945+438	US 995	RQQ	09 48 59.4	+43 35 18	16.45	-24.3	0.226	—	< -0.07
	2349-014	PKS 2349-01	LDQ	23 51 56.1	-01 09 13	15.45	-24.7	0.174	0.91	2.47
	1309+355	PG 1309+355	CDQ	13 12 17.7	+35 15 23	15.60	-24.7	0.184	0.31*	1.36
	1215+303	B2 1215+30	BL	12 17 52.0	+30 07 01	16.07	-24.8	0.237	8.0	2.63
2.	0514-005	1E 0514-0030	RQQ	05 16 33.5	-00 27 14	16.26	-25.1	0.291	—	< 0.06
	1004+130	PG 1004+130	LDQ	10 07 26.2	+12 48 56	15.28	-25.6	0.240	0.78	2.29
	1128+315	B2 1128+31	CDQ	11 31 09.4	+31 14 07	16.00	-25.3	0.289	0.62	2.43
3.	1252+020	Q 1252+0200	RQQ	12 55 19.7	+01 44 13	15.48	-26.2	0.345	—	-0.28
	0134+329	3C 48.0	LDQ	01 37 41.3	+33 09 35	16.62	-25.2	0.367	1.41	3.93
	1512+370	B2 1512+37	LDQ	15 14 43.0	+36 50 50	16.25	-25.6	0.370	1.17	3.57
	0851+202	OJ 287	BL	08 54 48.8	+20 06 30	15.91	-25.5	0.306	12.50	3.32
4.	1101+319	TON 52	RQQ	11 04 07.0	+31 41 11	16.00	-26.2	0.440	—	< -0.41
	1103-006	PKS 1103-006	LDQ	11 06 31.8	-00 52 53	16.39	-25.7	0.426	0.37	2.80
	1216-010	PKS 1216-010	CDQ	12 18 35.0	-01 19 54	16.17	-25.9	0.415	6.90**	2.34
	0735+178	PKS 0735+17	BL	07 38 07.4	+17 42 19	16.76	-25.4	>0.424	14.10	3.55
5.	1029+329	CSO 50	RQQ	10 32 06.0	+32 40 21	16.00	-26.7	0.560	—	< -0.64
	0709+370	B2 0709+37	LDQ	07 13 09.4	+36 56 07	15.66	-26.8	0.487	—	2.08
	0955+326	3C 232	CDQ	09 58 20.9	+32 24 02	15.88	-26.7	0.530	0.53	2.74
	0219+428	3C 66A	BL	02 22 39.6	+43 02 08	15.71	-26.5	0.444	11.70	2.83
6.	0748+294	QJ 0751+2919	RQQ	07 51 12.3	+29 19 38	15.00	-29.0	0.910	—	-0.68
	0350-073	3C 94	LDQ	03 52 30.6	-07 11 02	16.93	-27.2	0.962	1.42	3.07
	1308+326	B2 1308+32	CDQ	13 10 28.7	+32 20 44	15.61	-28.6	0.997	10.20	2.71
	0235+164	AO 0235+164	BL	02 38 38.9	+16 37 00	16.46	-27.6	0.940	14.90	3.29
7.	1017+279	TON 34	RQQ	10 19 56.6	+27 44 02	16.06	-29.8	1.918	—	< -0.49
	0012+305	B2 0012+30	LDQ	00 15 35.9	+30 52 30	16.30	-29.1	1.619	—	1.76
	1225+317	B2 1225+31	CDQ	12 28 24.8	+31 28 38	16.15	-30.0	2.219	0.16	2.26

[‡] log R is the ratio of the radio-to-optical flux densities calculated following Stocke et al. (1992)

[†] Optical polarization are from Wills et al. (1992) except those marked with * (Berriman et al. 1990) and ** (Hutsemekers & Lamy 2001)

Figure 6. Differential light curves of radio lobe-dominated quasars. The labels are as in Fig. 5.

Figure 6 *continued*

Figure 6 *continued*

Table 2. Results of INOV observations of QSOs. N is the total number of points, and T is the duration, of each observation. Status of INOV are denoted as V (for variables), PV (for probable variables) and NV (for non-variables). C_{eff} and ψ indicate the statistical significance and amplitude of variability. The variability timescale and periods are denoted as τ and P respectively. η_{obs} and δ_{obs} denote the accretion efficiency and doppler factor in the frame work of relativistic beaming models. The last column gives the references where DLCs are shown.

Set No.	Object	Date	N	T (hr)	INOV Status*	C_{eff}	ψ %	τ (hr)	P (hr)	η_{obs}	δ_{obs}	Ref. to DLCs	
1.	0945+438 (RQQ)	15.01.99	44	8.0	NV							Present work	
		26.02.00	31	6.3	NV							Present work	
		23.01.01	24	6.6	NV							Present work	
	2349-01 (LDQ)	13.10.01	34	6.8	V	3.6	2.2			0.02		SGSW03	
		17.10.01	39	7.6	V	3.1	1.5			0.02		SGSW03	
		18.10.01	40	7.7	V	3.2	1.6	5.0		0.02		SGSW03	
	1309+355 (CDQ)	25.03.99	39	6.7	NV							Present work	
		01.04.01	32	4.6	NV							Present work	
		02.04.01	41	5.2	NV							Present work	
	1215+303 (BL)	20.03.99	21	7.0	V	5.5	3.5	4.2			0.74	1.8	SSGW03
		25.02.00	28	5.9	NV								Present Work
		31.03.00	27	5.0	NV								Present Work
19.04.02		23	6.8	V	4.9	1.8	> 6.8			0.05	1.0	SSGW03	
09.12.01		25	5.3	NV								Present work	
2.	0514-005 (RQQ)	10.12.01	23	5.8	NV							Present work	
		19.12.01	35	7.5	NV							Present work	
		27.02.99	30	4.3	NV							Present work	
	1004+130 (LDQ)	16.02.99	36	6.5	NV								Present work
		29.03.00	21	3.8	NV								Present work
		30.03.00	26	4.6	NV								Present work
		18.02.01	42	5.5	NV								Present work
		24.03.01	50	6.4	NV								SGSW03
	1128+315 (CDQ)	18.01.01	31	5.7	NV								Present work
		09.03.02	27	8.2	NV								SGSW03
		10.03.02	28	8.3	NV								Present work
	3.	1252+020 (RQQ)	22.03.99	36	6.4	V	3.3	2.3					SGSW03
09.03.00			29	6.1	NV							Present work	
03.04.00			19	4.3	V	3.6	0.9	>4.3		0.04		SGSW03	
0134+329 (LDQ)		26.04.01	20	4.6	NV								Present work
		18.03.02	19	7.3	NV								Present work
		07.11.01	33	6.5	NV								Present work
		08.11.01	32	6.7	NV								Present work
		13.11.01	46	8.6	NV								Present work
1512+370 (LDQ)		23.03.02	24	7.0	NV								Present work
		27.03.02	28	7.0	NV								Present work
		21.04.02	11	4.3	V	2.8	2.6	0.4		0.53	1.60	SSGW03	
0851+202 (BL)		23.04.02	15	5.3	NV								Present work
	01.05.02	19	6.6	V	3.0	3.9	0.4	1.8,3.4,5.6	0.18	1.29	SSGW03		
	29.12.98	19	6.8	V	2.8	2.3	> 6.8		0.12	1.20	SSGW03		
	31.12.99	29	5.6	V	6.5	3.8	3.0		0.07	1.07	SSGW03		
	28.03.00	22	4.2	V	5.8	5.0	1.2		0.88	1.77	SSGW03		
	17.02.01	48	6.9	V	2.7	2.8	2.0	3.8	0.36	1.48	SSGW03		
4.	1101+319 (RQQ)	12.03.99	39	8.5	NV							Present work	
		04.04.00	22	5.6	NV							Present work	
		21.04.01	21	6.1	V	2.6	1.2	0.8		0.11	1.17	SGSW03	
	1103-006 (LDQ)	22.04.01	21	5.8	NV							Present work	
		17.03.99	23	3.8	NV							Present work	
		18.03.99	40	7.5	V	3.1	2.4	0.6		0.55	1.62	SGSW03	
		06.04.00	13	3.9	PV	2.1	1.2						SGSW03
		25.03.01	28	7.2	NV								SGSW03
		14.04.01	19	4.5	NV								Present work
		22.03.02	15	5.8	PV	2.2	0.7						SGSW03

Table 2. *Continued*

Set No.	Object	Date	N	T (hr)	INOV Status	C_{eff}	ψ %	τ (hr)	P (hr)	η_{obs}	δ_{obs}	Ref. to DLCs	
4.	1216–010 (CDQ)	11.03.02	22	8.0	V	3.2	7.3	1.8	3.2	0.29	1.42	SSGW03	
		13.03.02	24	8.5	V	2.6	3.8	1.2	2.2	0.16	1.26	SSGW03	
		15.03.02	11	3.9	V	3.9	5.5	1.0	2.2	0.77	1.73	SSGW03	
	0735+178 (BL)	16.03.02	22	8.2	V	6.6	14.1	> 8.2					SSGW03
		26.12.98	49	7.8	NV								SGSW03
		30.12.99	65	7.4	NV								Present work
5.	1029+329 (RQQ)	25.12.00	43	6.0	NV							Present work	
		24.12.01	43	7.3	V	2.8	1.0	> 8.1		0.05	1.00	SSGW03	
		13.03.99	45	8.4	—								
	0709+370 (LDQ)	02.03.00	19	5.0	NV								Present work
		05.04.00	19	5.3	V	4.3	1.3	>6.2		0.13	1.21		SGSW03
		23.03.01	20	5.8	NV								Present work
0955+326 (CDQ)	06.03.02	31	8.5	NV								SGSW03	
	08.03.02	17	6.8	V	2.8	1.1						SGSW03	
	20.01.01	29	6.5	NV								Present work	
0219+428 (BL)	21.01.01	29	6.2	NV								Present work	
	25.01.01	31	7.1	NV								Present work	
	20.12.01	49	7.9	V	3.1	1.4	4.4	7.0	0.007			SGSW03	
6.	0748+294 (RQQ)	21.12.01	48	7.5	NV							Present work	
		19.02.99	36	6.5	NV							Present work	
		03.03.00	37	6.3	NV							Present work	
	0350–073 (LDQ)	05.03.00	34	6.9	PV	2.2	0.7						SSGW03
		14.11.98	118	6.5	V	6.0	5.4	> 6.5		1.04	1.80		SSGW03
		13.11.99	123	5.7	V	> 6.6	5.5	> 5.9		4.91	2.50		SSGW03
1308+326 (CDQ)	24.10.00	73	9.1	V	5.8	4.3	> 9.1		1.39	1.94		SSGW03	
	26.10.00	82	10.1	V	3.5	3.2	4.9		1.14	1.87		SSGW03	
	01.11.00	103	9.0	V	2.9	2.2	3.9		0.26	1.39		SSGW03	
0235+164 (BL)	24.11.00	71	5.1	NV								Present work	
	01.12.00	59	5.1	V	>6.6	8.0	> 5.1		2.14	2.12		SSGW03	
	14.12.98	22	7.6	NV								Present work	
7.	1017+279 (RQQ)	13.01.99	56	8.3	NV							Present work	
		09.12.99	26	5.1	NV							Present work	
		24.11.00	28	5.4	NV							Present work	
	0012+305 (LDQ)	01.12.00	32	6.0	NV								SGSW03
		25.12.01	30	5.4	NV								SGSW03
		14.11.01	31	6.6	NV								Present work
1225+317 (CDQ)	15.11.01	26	5.5	NV								Present work	
	18.11.01	25	5.7	NV								Present work	
	23.03.99	17	6.0	—									
7.	1017+279 (RQQ)	26.04.00	16	5.6	NV							Present work	
		03.05.00	19	6.7	—								
		17.03.02	19	7.7	V	3.1	3.4	1.2,4.4		5.39	2.55		SSGW03
	0235+164 (BL)	20.04.02	14	5.8	NV								Present work
		02.05.02	15	5.1	NV								Present work
		13.11.98	36	4.4	—								
1017+279 (RQQ)	12.11.99	39	6.6	V	>6.6	12.8	3.6		2.48	2.18		SSGW03	
	14.11.99	34	6.2	V	3.2	10.3	3.4		1.23	1.90		SSGW03	
	22.10.00	39	7.9	V	2.6	7.6			1.71	2.03		SSGW03	
7.	1017+279 (RQQ)	28.10.00	29	6.8	—								
		14.03.99	43	7.3	NV								Present work
		14.01.00	33	7.1	NV								Present work
	0012+305 (LDQ)	27.02.00	33	8.1	NV								Present work
		18.01.01	17	3.6	NV								Present work
		20.01.01	14	3.2	NV								Present work
1225+317 (CDQ)	24.01.01	14	2.9	NV								Present work	
	14.10.01	20	5.7	NV								Present work	
	21.10.01	22	5.7	NV								SGSW03	
1017+279 (RQQ)	22.10.01	24	6.2	NV								Present work	
	07.03.99	49	6.6	NV								Present work	
	07.04.00	23	6.0	NV								Present work	
1017+279 (RQQ)	20.04.01	34	7.4	NV								Present work	

Table 3. Results for INOV and LTOV of the QSOs observed in this program

Object	Type	Date	Q-S1 (mag)	Q-S2 (mag)	Q-S3 (mag)	S1-S2 (mag)	S1-S3 (mag)	S2-S3 (mag)
2349-014	LDQ	17.10.01	0.000	0.000	0.000	0.000	0.000	0.000
		13.10.01	0.030	0.035	0.047	0.005	0.016	0.011
		18.10.01	0.046	0.048	0.049	0.002	0.002	-0.001
1309+355	LDQ	01.04.01	0.000	0.000	0.000	0.000	0.000	0.000
		02.04.01	0.004	0.003	0.000	0.000	-0.004	-0.004
		25.03.99	0.107	0.097	0.128	-0.010	0.021	0.031
1215+303	BL	25.04.01	0.000		0.000			0.000
		19.04.01	0.108		0.098			-0.010
		31.03.00	0.201		0.206			0.006
		25.02.00	0.344		0.322			-0.022
0514-005	RQ	20.03.99	0.522		0.468			-0.054
		19.12.01	0.000	0.000	0.000	0.000	0.000	0.000
		09.12.01	0.004	0.014	0.006	0.010	0.002	-0.008
1004+130	LDQ	10.12.01	0.011	0.007	0.009	-0.004	-0.002	0.002
		18.02.01	0.000	0.000		0.000		
		24.03.01	-0.003	0.001		0.004		
		29.03.00	0.002	0.005		0.003		
		30.03.00	0.021	0.028		0.007		
		16.03.99	0.077	0.089		0.012		
1128+310	CDQ	27.02.99	0.081	0.099		0.018		
		18.01.01	0.000	0.000	0.000	0.000	0.000	0.000
		09.03.02	0.135	0.136	0.130	0.001	-0.005	-0.006
		10.03.02	0.037	0.136	0.132	-0.001	-0.006	-0.004
1252+020	RQQ	09.03.00	0.000	0.000		0.000		
		03.04.00	0.006	0.002		-0.003		
		18.03.02	0.087	0.082		-0.005		
0134+329	LDQ	26.04.01	0.177	0.183		0.006		
		07.11.01	0.000	0.000	0.000	0.000	0.000	0.000
		08.11.01	0.002	-0.001	-0.001	-0.003	-0.004	0.000
1512+370	LDQ	13.11.01	0.008	0.016	0.013	0.008	0.005	-0.003
		21.04.02	0.000	0.000	0.000	0.000	0.000	0.000
		23.04.02	0.031	0.025	0.023	-0.005	-0.008	-0.002
		01.05.02	0.033	0.027	0.030	-0.006	-0.003	0.003
		27.03.02	0.054	0.048	0.047	-0.005	-0.007	-0.002
0851+202	BL	23.03.02	0.085	0.082	0.082	-0.003	-0.003	0.001
		31.12.99	0.000	0.000	0.000	0.000	0.000	0.000
		29.12.98		0.601	0.695			0.094
		28.03.00	0.936	0.928	0.906	-0.009	-0.031	-0.020
1101+319	RQQ	17.02.01	1.631	1.628	1.624	-0.004	-0.007	-0.003
		04.04.00		0.000	0.000			0.000
		22.04.01		0.041	0.042			0.000
		21.04.01		0.052	0.050			-0.003
		12.03.99		0.193	0.184			-0.009
1103-006	LDQ	06.04.00	0.000	0.000	0.000			
		17.03.99	0.018	0.018	-0.004			
		18.03.99	0.021	0.021	-0.001			
		14.04.01	0.316	0.314	-0.003			
		25.03.01	0.318	0.314	-0.005			
1216-010	CDQ	22.03.02	0.329	0.324	-0.006			
		15.03.02	0.000	0.000		0.000		
		11.03.02	0.087	0.085		-0.001		
		13.03.02	0.106	0.102		-0.003		
		16.03.02	0.140	0.135		-0.004		

Table 3. *Continued*

Object	Type	Date	Q-S1 (mag)	Q-S2 (mag)	Q-S3 (mag)	S1-S2 (mag)	S1-S3 (mag)	S2-S3 (mag)
0735+178	BL	26.12.98	0.000		0.000		0.000	
		30.12.99	0.457		0.465		0.008	
		24.12.01	0.720		0.715		-0.005	
		25.12.00	1.145		1.147		0.002	
0709+370	LDQ	20.01.01	0.000	0.000	0.000	0.000	0.000	0.000
		25.01.01	0.005	0.002	0.003	-0.003	-0.002	0.001
		21.01.01	0.004	0.005	0.006	0.001	0.002	0.000
		21.12.01	0.025	0.017	0.021	-0.008	-0.004	0.004
		20.12.01	0.040	0.029	0.033	-0.011	-0.008	0.004
0955+326	CDQ	19.02.99	0.000		0.000		0.000	
		03.03.00	0.044		0.057		0.013	
		05.03.00	0.047		0.060		0.013	
0219+428	BL	24.10.00	0.000		0.000		0.000	
		26.10.00	0.255		0.256		0.001	
		24.11.00	0.277		0.281		0.003	
		01.11.00	0.331		0.330		-0.001	
		13.11.99	0.449		0.449		0.000	
		01.12.00	0.622		0.631		0.010	
0748+294	BL	14.11.98	0.691		0.684		-0.007	
		13.01.99	0.000	0.000	0.000	0.000	0.000	0.000
		25.12.01	0.231	0.221	0.214	-0.010	-0.017	-0.007
		24.11.00	0.231	0.221	0.210	-0.009	-0.021	-0.012
		01.12.00	0.237	0.226	0.209	-0.010	-0.028	-0.017
		14.12.98	0.239	0.236	0.207	-0.002	-0.031	-0.029
0350-073	LDQ	09.12.99	0.242	0.238	0.234	-0.004	-0.008	-0.004
		14.11.01	0.000	0.000	0.000	0.000	0.000	0.000
		18.11.01	0.000	-0.001	-0.001	0.000	0.000	0.000
1308+326	CDQ	15.11.01	0.000	0.005	0.006	0.002	0.003	0.002
		26.04.00	0.000	0.000		0.000		
		03.05.00	0.016	0.009		-0.006		
		23.03.99	0.204	0.203		0.000		

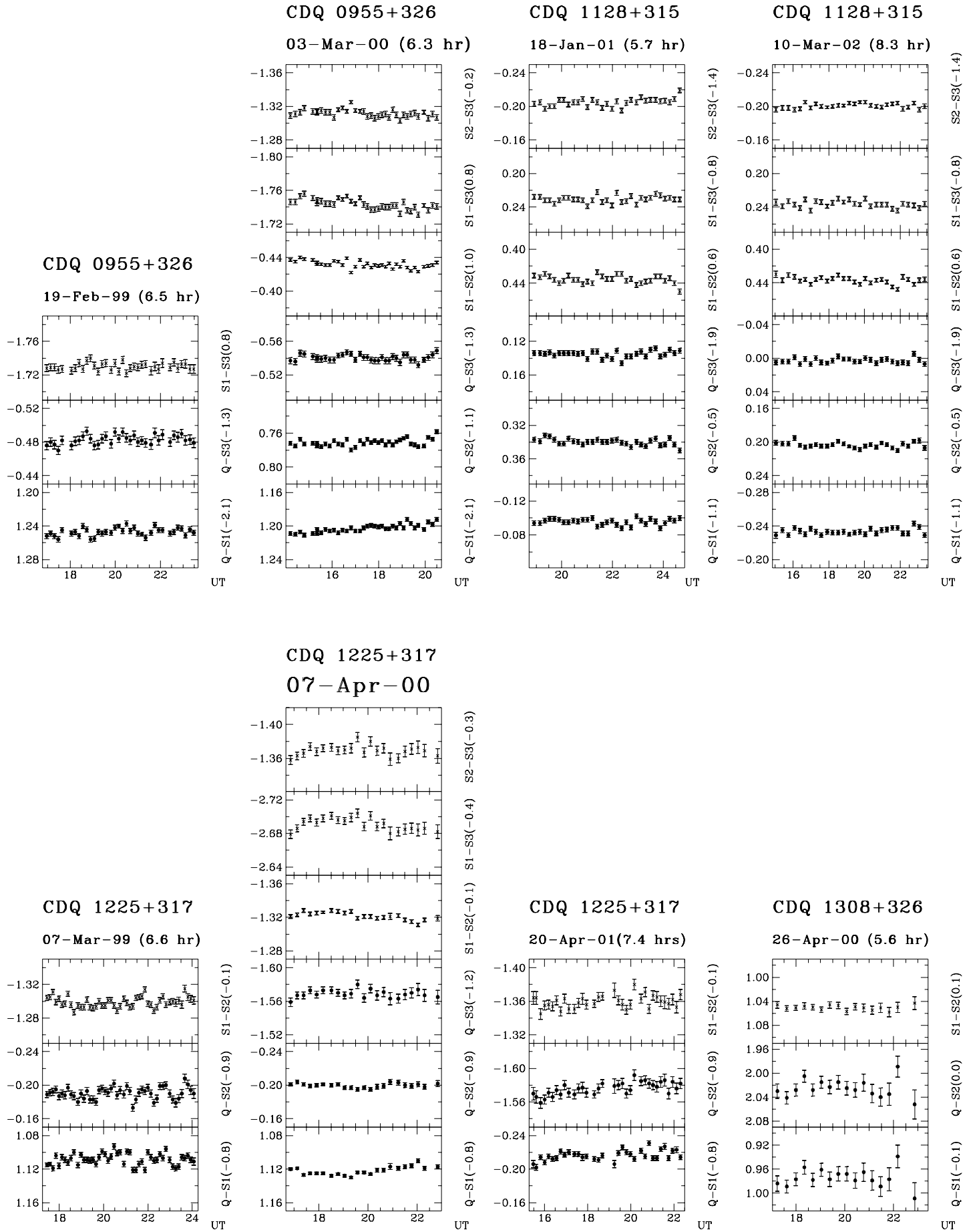


Figure 7. Differential light curves of radio core-dominated quasars. The labels are as in Fig. 5.

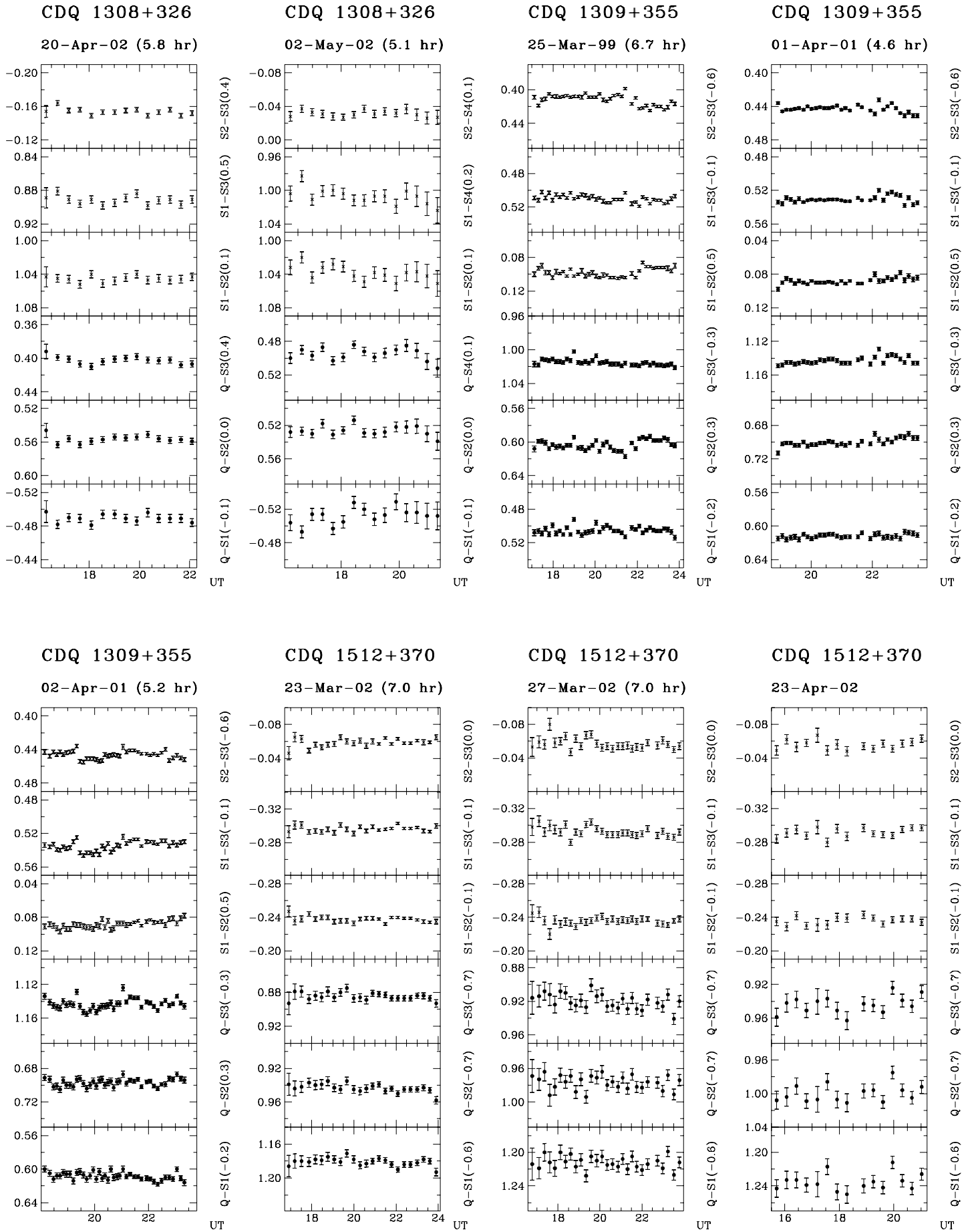


Figure 7 continued

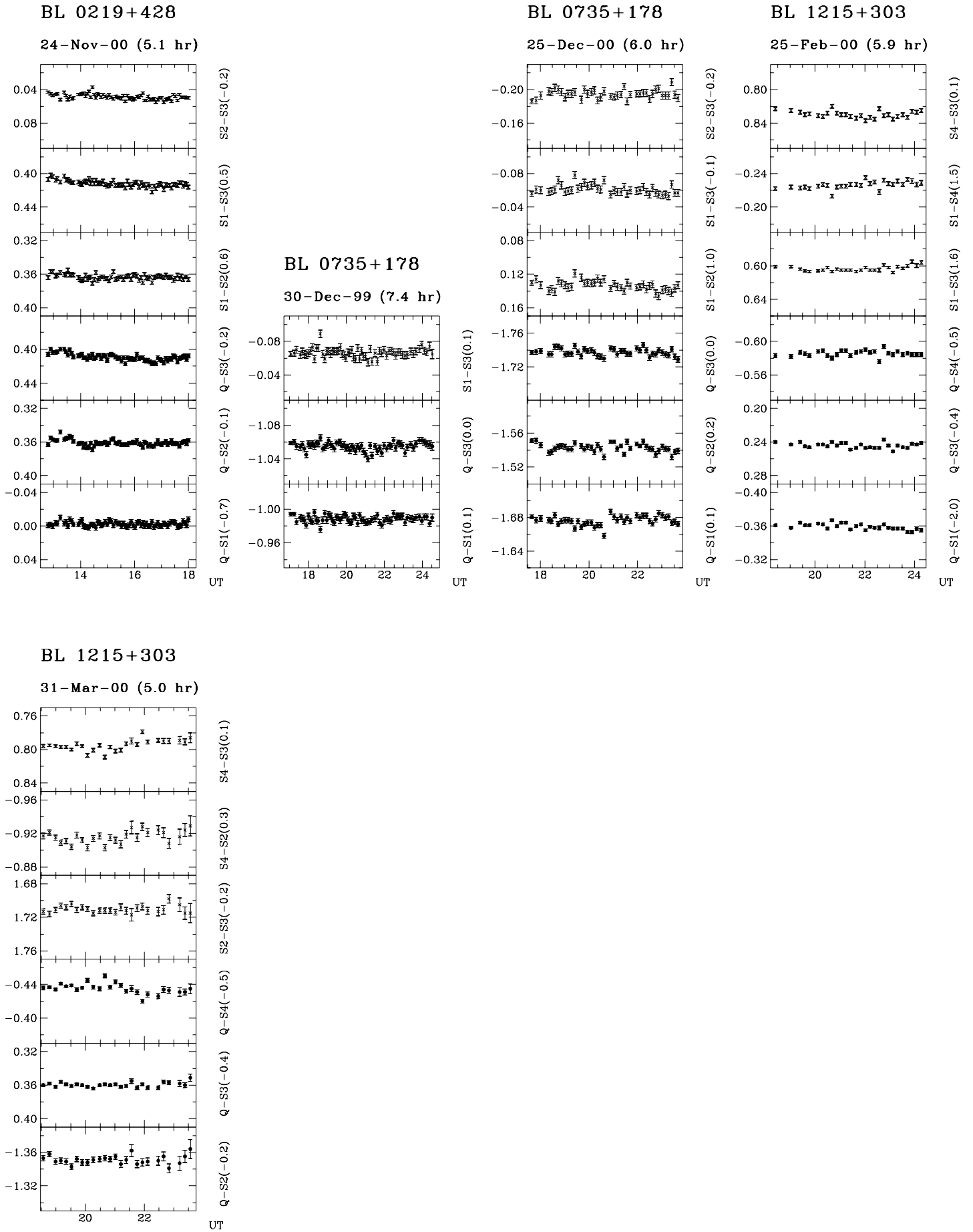
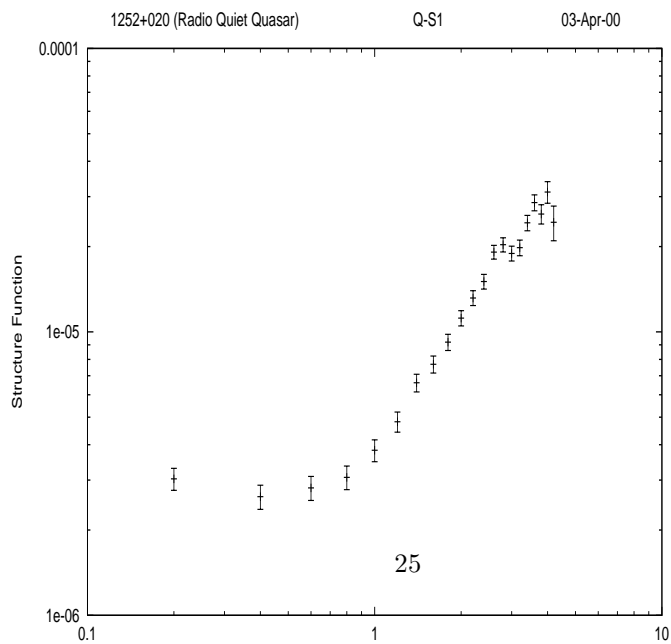
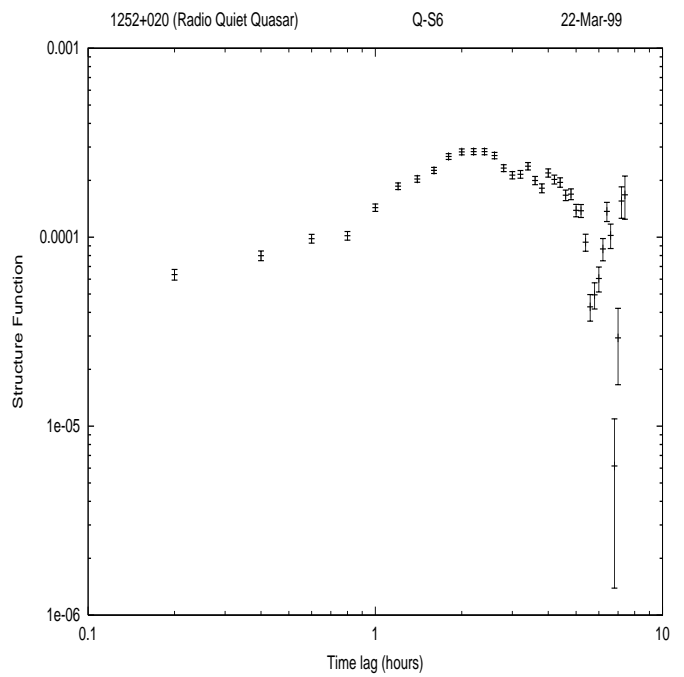
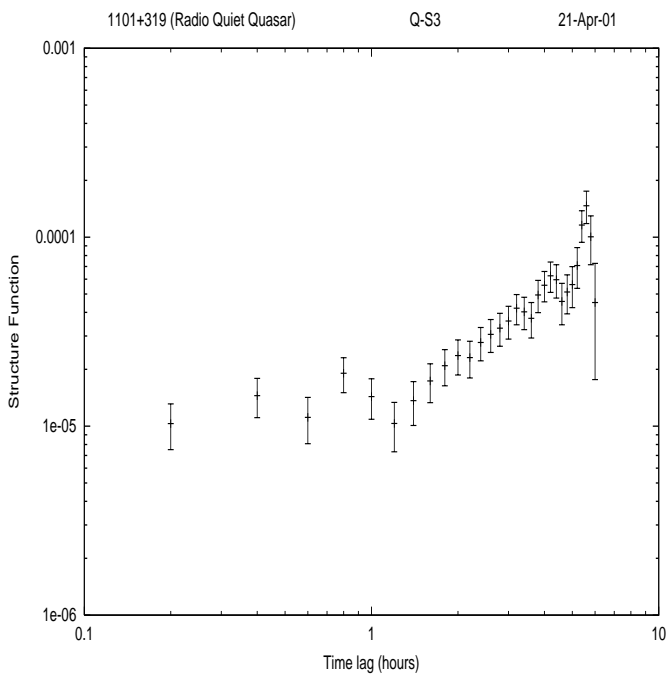
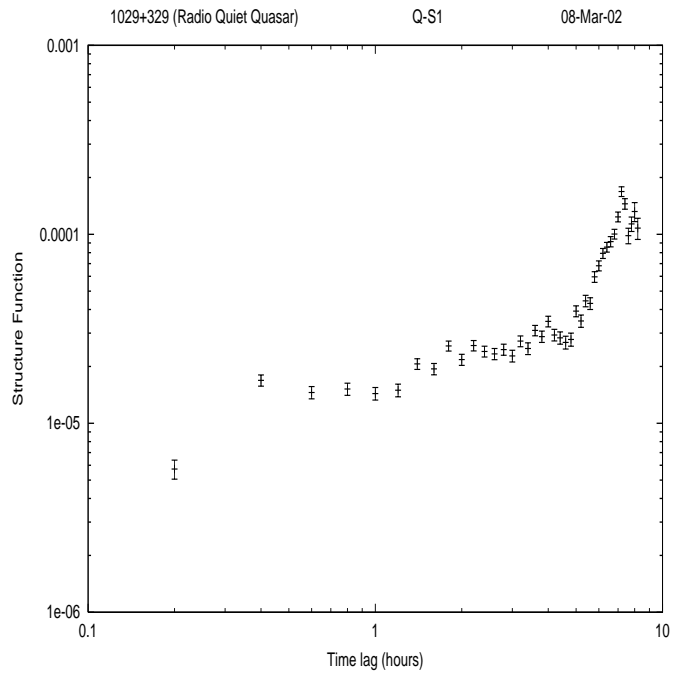
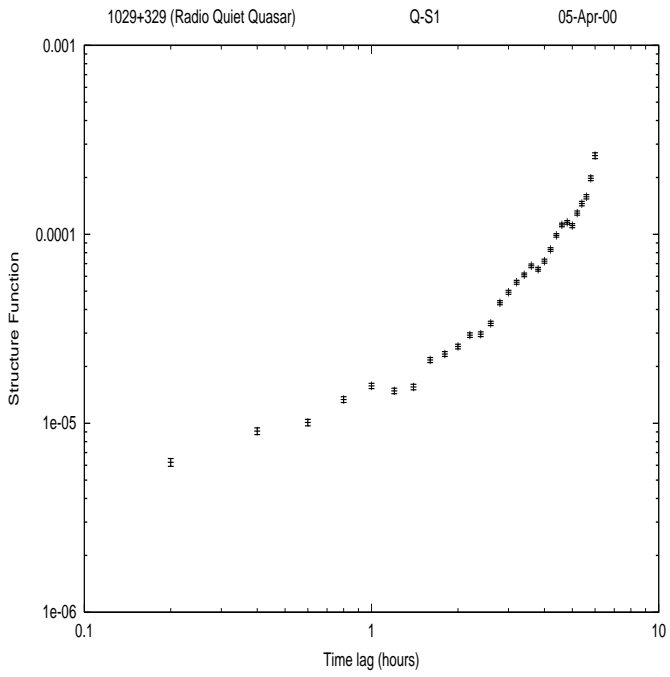


Figure 8. Differential lightcurves of BL lacertae objects. The labels are as in Fig. 5.



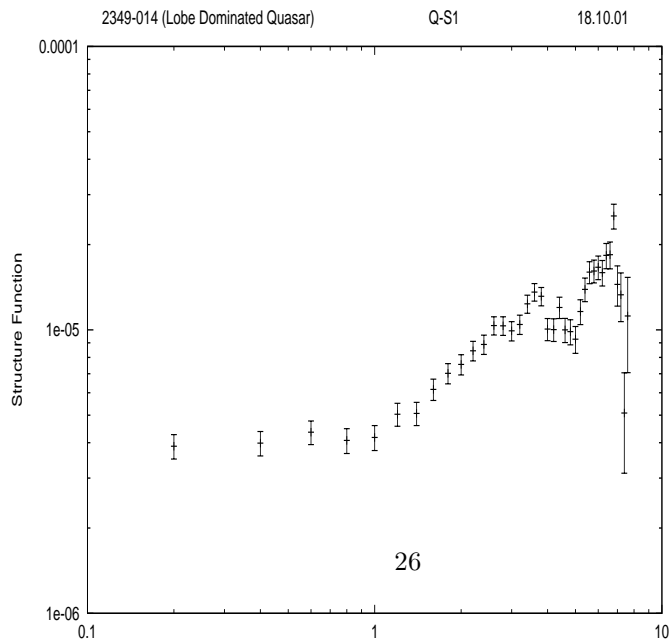
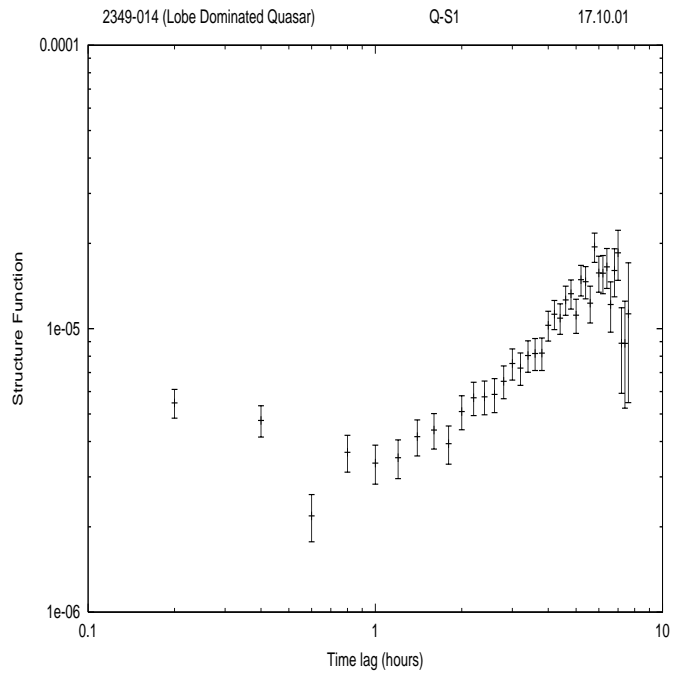
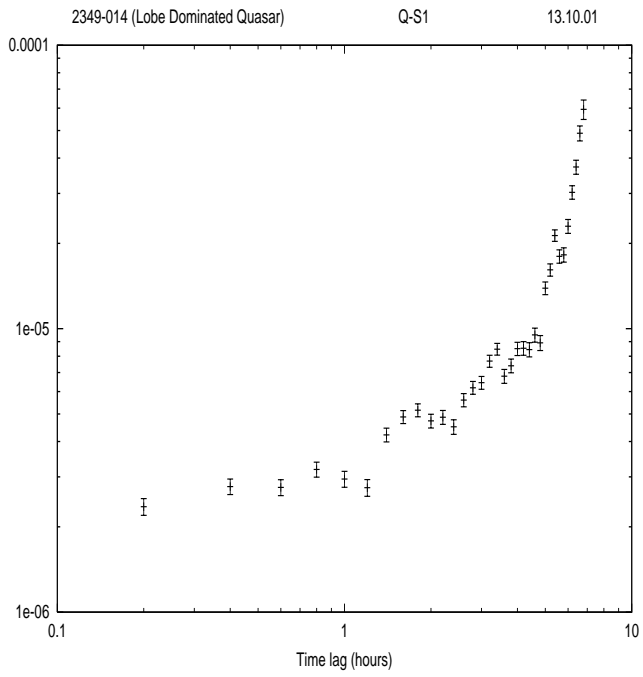
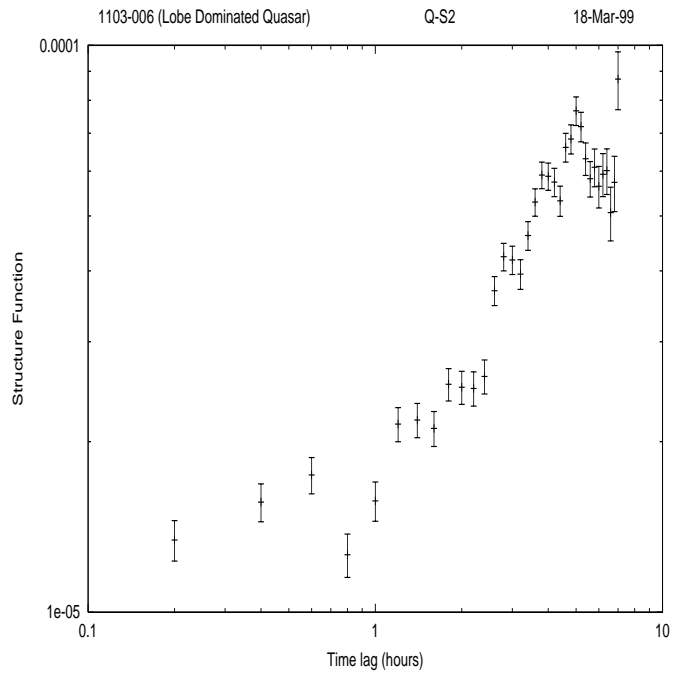
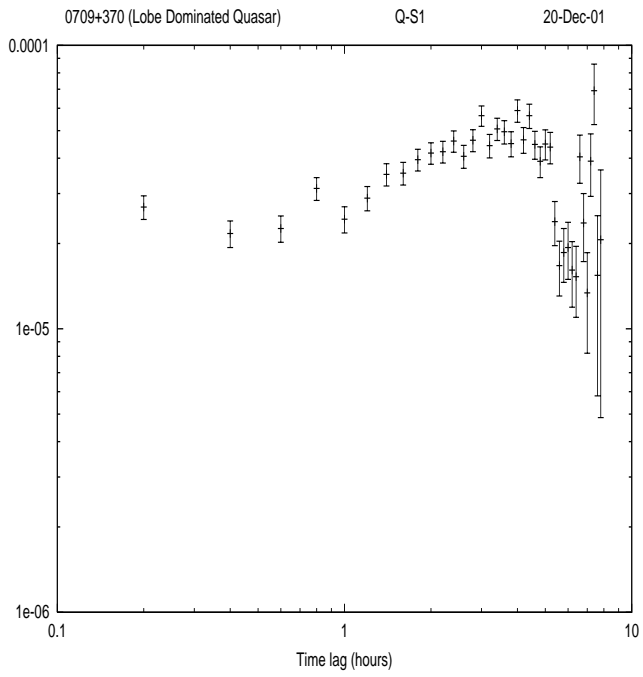


Figure 11. Long term variability of 1 core dominated quasar and 5 lobe dominated quasars observed in this programme.

Figure 12. Long term variability of 6 radio-quiet quasars observed in this programme,

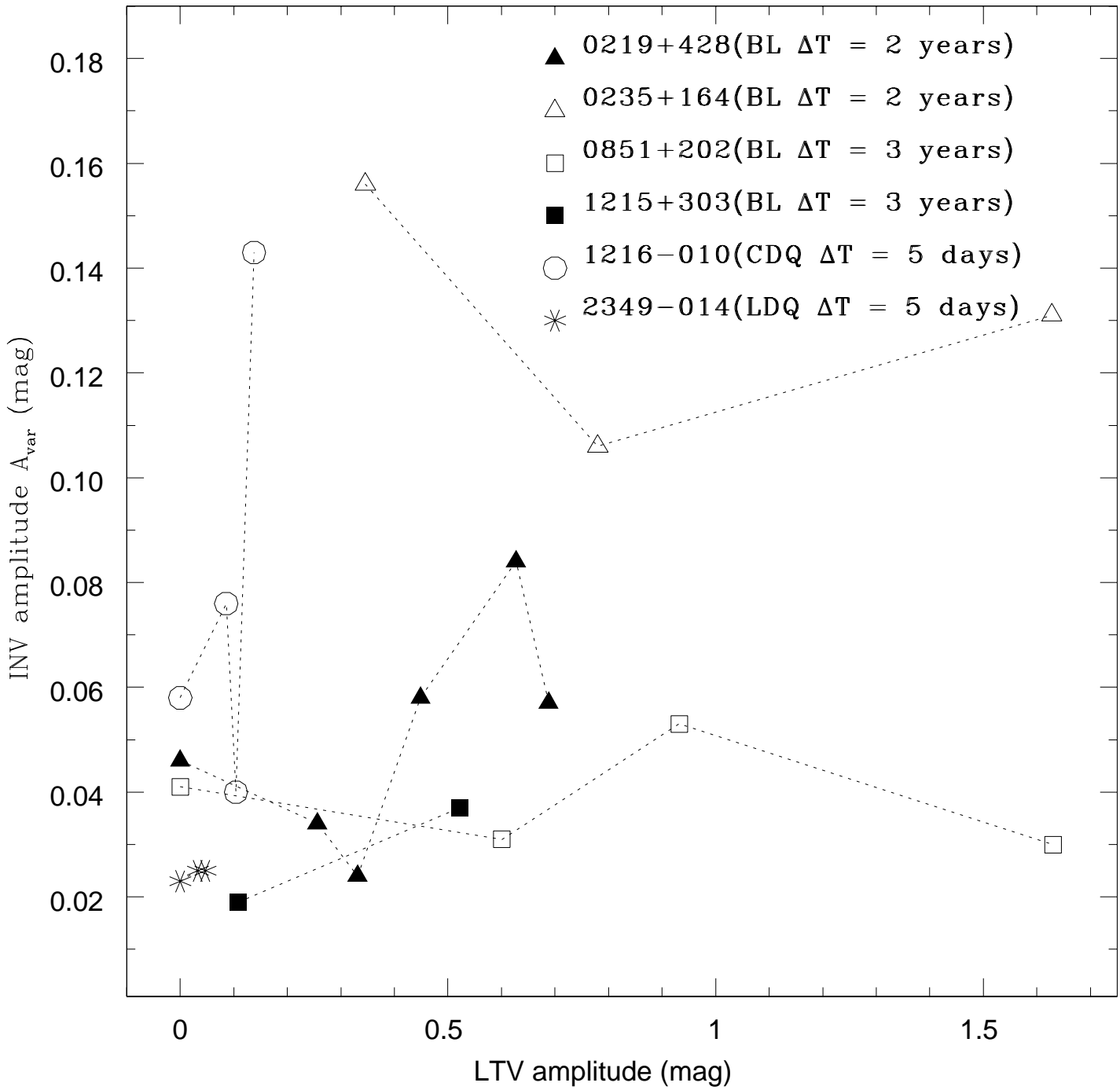


Figure 13. Comparison of INOV against LTOV.

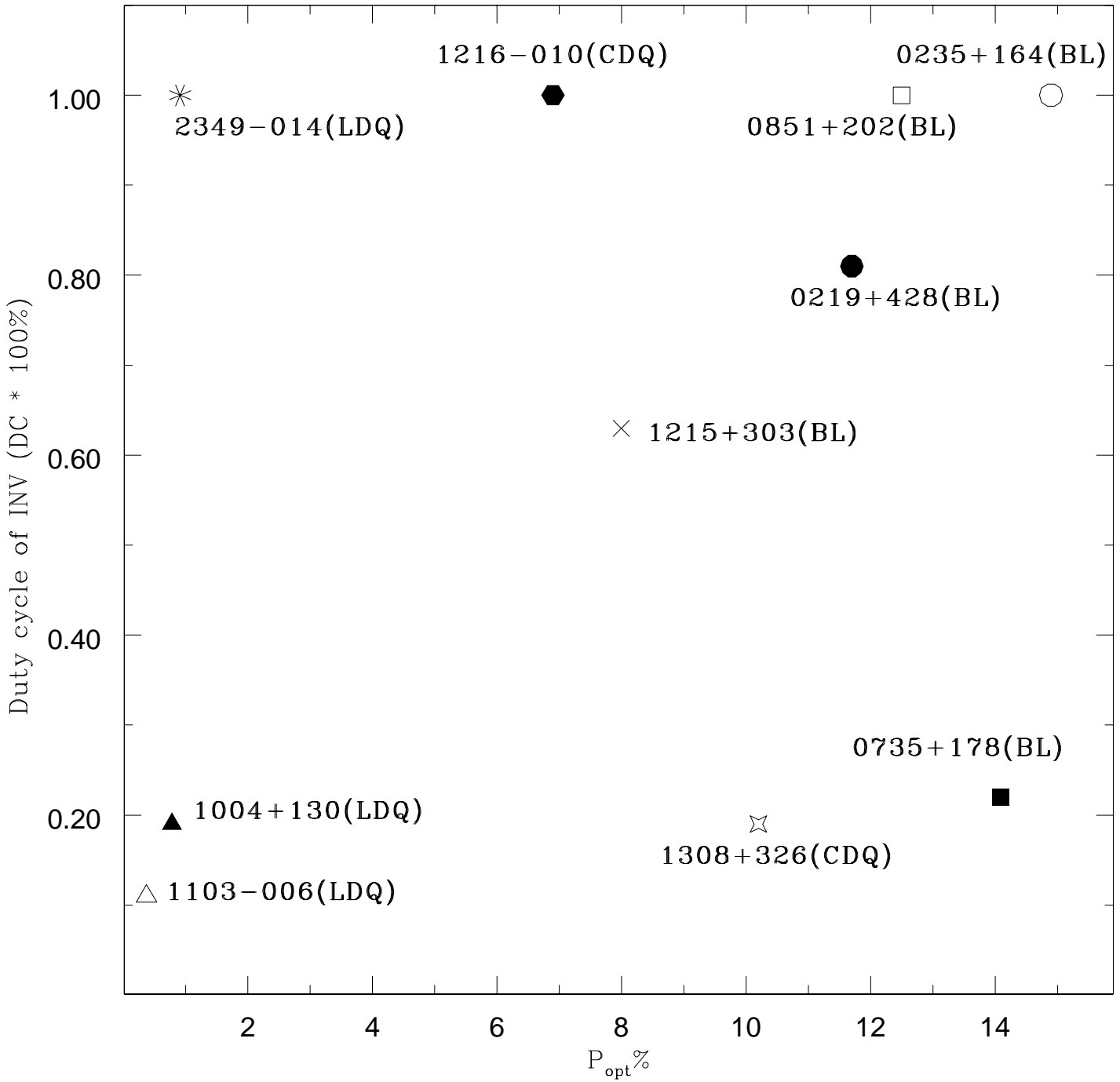


Figure 14. INOV duty cycles for objects which show INOV against their optical polarization.